



MACQUARIE
University

Macquarie University PURE Research Management System

This is the Accepted Manuscript version of the following article:

Zhang, S., De Leon Rodriguez, L.M., Lacey, E., Piggott, A.M., Leung, I.K.H. and Brimble, M.A. (2017) Cyclization of linear tetrapeptides containing N-nethylated amino acids by using 1-propanephosphonic acid anhydride, *European Journal of Organic Chemistry*, Vol. 2017, No. 1, pp. 149-158.

which has been published in final form at:

<https://doi.org/10.1002/ejoc.201601016>

Publisher: Wiley

Copyright: 2017 Wiley-VCH Verlag GmbH & Co. KGaA

Cyclisation of Linear Tetrapeptides Containing *N*-Methylated Amino Acids Using 2-Propanephosphonic Acid Anhydride

Shengping Zhang,^[a] Luis M. De Leon Rodriguez,^[b] Ernest Lacey,^[c] Andrew M. Piggott,^[d] Ivanhoe K. H. Leung^[a] and Margaret A. Brimble^{*[a,b]}

Abstract: The cyclisation of linear tetrapeptides of sequence H-MMePhe-Xaa¹-NMePhe-Xaa²-OH (where Xaa¹ = Xaa² = Ile, Val or Leu; Xaa¹ = Val and Xaa² = Ile or Leu) using 2-propanephosphonic acid anhydride is reported. An unanticipated finding was that cyclisation gives cyclotetrapeptide conformers (kinetic products), which are highly prone to hydrolysis and that slowly interconvert into the more stable *trans,cis,trans,cis* conformers (thermodynamic products).

Introduction

Cyclotetrapeptides are an uncommon family of microbial metabolites, with fewer than thirty analogues reported in the literature. Despite this chemical “under-representation” in nature, cyclotetrapeptides display diverse pharmacology as phytotoxic peptides,^[1] an inhibitor of lipopolysaccharide-induced nitric oxide production,^[2] antibacterial peptides,^[3] inhibitors of histone deacetylase,^[4] inhibitors of glycine transporter type 1^[5] and cardiac calcium channel blockers.^[6]

An important class of cyclotetrapeptides involves peptides containing unnatural *N*-methylated amino acids (*N*-Me-aa) within their sequence. Some examples of these type of peptides are briefly described below.

Tentoxin (**1**) (Figure 1), a phytotoxic cyclic tetrapeptide extracted from the fungus *Alternaria alternata*, contains a pair of alternating *N*-Me-aa, one of which includes a characteristic α,β -dehydro Phe amino acid.^[7]

Hirsutide (**2**) (Figure 1), a cyclotetrapeptide containing two *N*-Me-Phe residues, was isolated from the entomopathogenic fungus *Hirsutiella* sp. that infected a spider.^[8] Additionally, three cyclotetrapeptides (**3–5**), structurally related to hirsutide, were identified from the crude fermentation extract of the fungus *Onychocola sclerotica* (hereinafter referred to as onychocins),^[6]

and more recently, onychocin A (**4**) and an inseparable complex of onychocins B (**5**) and D (**7**) (Figure 1) were found as the major metabolites of the fungus, *Aspergillus hancockii* sp. nov.^a The onychocins showed important activity as cardiac calcium channel blockers

Endolides A and B, which contain two units of the unusual *N*-Me 3-(3-furyl)alanine amino acid, isolated from *Stachylidium* sp.^[9] and the pseudoxylallemycins, which contain two tyrosines modified with an allenic ether C-4 building block, from *Pseudoxylaria* sp. X802^[10] provide more examples of the role of rare and non-conventional amino acids in the cyclotetrapeptide scaffold.

While our understanding of the function of the cyclotetrapeptides in nature is still evolving, there is a pressing need for simple synthetic protocols to produce cyclotetrapeptide scaffolds.

It is well documented that all L-cyclotetrapeptides lacking turn promoting residues (e.g. proline, D- or *N*-Me-aa) are difficult to synthesize given the geometric constraints needed to be overcome to form the cyclic structure. This can be exemplified with the tyrosine inhibitor cyclo(Pro-Val-Pro-Tyr),^[11] whose synthesis has been elusive to date despite containing two Pro residues within its structure. Remarkably, the advent of methodologies based on ring contraction strategies or the use of pseudoproline amino acid precursors has provided important tools for the synthesis of the highly strained cyclotetrapeptides.^[12] Moreover, even for linear peptides containing several turn-promoting amino acids, the success of cyclisation is still sequence-dependent.^[13] For instance, the cyclo(DPro-DPro-Pro-Pro) peptide could only be obtained when starting from H-DPro-Pro-Pro-DPro-COOH.^[14]

Cyclotetrapeptides containing *N*-Me-aa are particularly attractive pharmacological leads given their compliance with Lipinski's rules, such as not containing more than 5 hydrogen bond donors and not more than 10 hydrogen bond acceptors.^[15] However, problems frequently encountered during the synthesis of peptides containing *N*-Me-aa are: deletions, given the difficult coupling to the secondary amino group of the *N*-Me-aa; peptide bond cleavage (particularly observed for peptides containing consecutive *N*-Me-aa)^[16] and diketopiperazine formation.^[17] Thus, cyclotetrapeptides containing one or two non-consecutive *N*-Me-aa are expected to be the least problematic from a synthetic point of view and the most stable. Moreover, reports on the synthesis of these kinds of systems are scarce. In early reports the synthesis of cyclotetrapeptides containing *N*-Me-aa was accomplished by preparing the linear peptide by solution phase protocols followed by cyclisation of the corresponding 2,4,5-trichlorophenyl (Tcp) or pentafluorophenyl (Pfp) peptide ester.

- [a] S. Zhang, M.A. Brimble
School of Chemical Sciences, The University of Auckland,
23 Symonds St, Auckland, 1142, New Zealand
E-mail: m.brimble@auckland.ac.nz
- [b] LM De Leon Rodriguez, M.A. Brimble
Maurice Wilkins Centre for Molecular Biodiscovery, The University of
Auckland
Auckland, 1142, New Zealand
- [c] E. Lacey
Microbial Screening Technologies
Building AC, 28-54 Percival Rd., Smithfield, NSW 2164, Australia
- [d] A.M. Piggott
Department of Chemistry and Biomolecular Sciences
Macquarie University, NSW 2109, Australia

Supporting information for this article is given via a link at the end of the document.

^a J. Pitt, **personal communication**, December 2014

Typically, the cyclisation step was carried out under high dilution conditions in boiling pyridine/solvent mixtures in the presence of base (e.g. *N,N*-dimethyl-4-aminopyridine and *N,N*-diisopropylethylamine (DIPEA)). However, the yields of the cyclisation step were usually poor.^[18]

The cyclisation step of the linear peptide precursor of tentoxin (**1**) has been reported under a variety of conditions, allowing one to compare the effectiveness of different cyclisation protocols.^[19] Cyclisation yields varied from poor (18%) using the Tcp peptide ester^[19a] to excellent (73% and 81%) when employing the conventional coupling agents *O*-(benzotriazol-1-yl)-*N,N,N',N'*-tetramethyluronium hexafluorophosphate (HBTU) and *O*-(7-azabenzotriazol-1-yl)-*N,N,N',N'*-tetramethyluronium hexafluorophosphate (HATU) in the presence of base in DMF at room temperature.^[19e]

The synthesis of hirsutide (**2**) has been reported.^[20] The cyclisation of the Pfp ester of the linear peptide precursor of **2** (H-Phe-MMePhe-Val-MMePhe-OH) was carried out at low temperature and high peptide concentration giving **2** in high yield (81%). These conditions are opposite to what has been reported for other cyclotetrapeptides which were prepared from their corresponding Pfp ester at high temperature under high dilution to minimize dimerization.^[18]

As already noted the need for new strategies to prepare cyclotetrapeptides is of paramount importance. In this work the onychocins were judiciously selected as an informative template to provide the natural products (**3**, **4**, **5**, **7**) and closely related analogue (**6**) for biological evaluation (Figure 1).

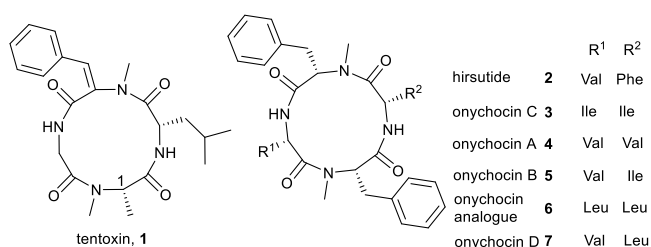


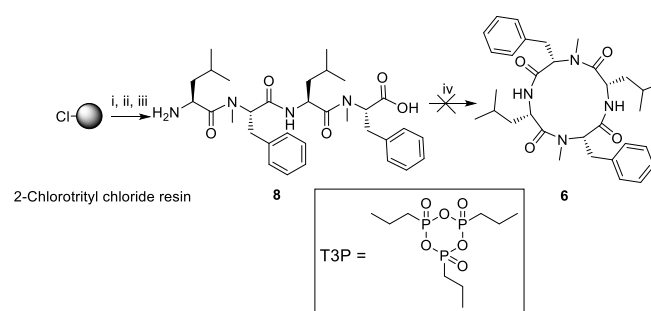
Figure 1. *N*-methylated cyclotetrapeptides

Results and Discussion

We are interested in exploring new methodologies for the cyclisation of linear tetrapeptides and considered that 2-propanephosphonic acid anhydride (T3P) may offer advantages over existing condensing reagents. It is known that T3P gives superior results compared to HATU with respect to maintaining the stereochemistry of the cyclisation site of linear pentapeptides containing sterically hindered amino acids.^[21] Additionally, to the best of our knowledge T3P has not been used in the cyclisation of linear tetrapeptides. Thus, considering the successful reported synthesis of hirsutide (**2**) from its linear precursor H-Phe-MMePhe-Val-MMePhe-OH,^[20] we first proceeded with the cyclisation of the linear peptide H-Leu-MMePhe-Leu-MMePhe-OH (**8**) precursor of onychocin **6** (synthesized by conventional solid phase peptide synthesis protocols on a polystyrene resin

derivatized with a 2-chlorotrityl chloride linker (Scheme 1)), using 5 equiv. of T3P, 6 equiv. of DIPEA in CH₂Cl₂/DMF (1:1) for 24 hours at room temperature at 1 mmol peptide concentration. Interestingly, the linear peptide dimer and the corresponding cyclic dimeric octapeptide were the only products observed by RP-HPLC-UV-ESIMS.

On the other hand, when starting from H-MMePhe-Leu-MMePhe-Leu-OH (**9**) under the same conditions using T3P as the cyclisation agent, the desired cyclic tetrapeptide **6** was obtained in low yield (15%) together with a small proportion of the cyclopeptide containing the epimerized C-terminal amino acid (**6***) (Scheme 2 and Figure 2A) (**6*** was independently synthesized to enable its thorough characterization). This finding seems to conflict with the analogous reported synthesis of hirsutide (**2**).



Scheme 1. Initial approach for the synthesis of **6**. Reagents and conditions: (i) Fmoc-*N*-Me-Phe-OH, CH₂Cl₂, DIPEA, rt, 1 h; (ii) Fmoc-SPPS (Fmoc deprotection: 20% piperidine in DMF, rt, 2 × 5 min; coupling: Fmoc-amino acid, HATU, DIPEA, DMF, rt, 45 min; iii) HFIP/ CH₂Cl₂ (1:4), rt, 1 h; iv) T3P, CH₂Cl₂/DMF (1:1), DIPEA, rt, 24 h.

The yield of **6** was similar to that reported for analogous systems.^[18] Furthermore, the cyclisation was not complete since the linear peptide precursor **9** and the corresponding C-terminal epimerized linear peptide **9*** were also detected by RP-HPLC (Scheme 2 and Figure 2A).

The cyclotetrapeptide **6** was fully characterized by RP-HPLC, HRMS, NMR (¹H, ¹³C, COSY, HSQC and NOESY), IR (see supporting information Figures S16-S24) and optical rotation.

The NOESY spectrum of **6** showed a *trans* configuration for the *N*-Me-Phe-Leu peptide bond (CONH) as evidenced by a correlation between the C^αH (*N*-Me-Phe) and NH (Leu) protons (see supporting information Figures S22-S23). Also, a correlation between the C^αH protons of *N*-Me-Phe and Leu was observed, which is indicative of a *cis* configuration for the Leu-*N*-Me-Phe peptide bond (CONCH₃) (supporting information Figure S23) (Note that a correlation between CH₃ (*N*-Me-Phe) and C^αH (Leu) will indicate a *trans* configuration).^[22]

Therefore, we concluded that **6** exists in a *trans,cis,trans,cis* (*tctc*) conformation in solution, which corresponds to the most stable structure reported for analogous systems.^[23]

In order to determine optimal conditions for the cyclisation of **9** with T3P, the effect of the solvent, base strength and peptide concentration was further studied. The cyclisation of **9** to **6** was

observed when the reaction was carried out for 24 hours in a mixture of CH₂Cl₂/DMF (1:1) or in CH₂Cl₂ at room temperature, although the reaction was slower and low yielding in the later stages (see supporting information Figure S25). However, when the reaction was carried out in DMF or EtOAc under similar conditions no product formation took place but epimerization of the starting material was observed (see supporting information Figure S26). Similarly, neither cyclisation nor starting material C-terminal epimerization occurred with weaker bases such as collidine or pyridine and only starting material epimerization was detected using *N,N*-dimethyl-4-aminopyridine. An increase in the number of equiv. of T3P or base had no positive effect on the yield of the desired product but rather a decrease in yield of **6** or an increase in **9*** were observed, respectively. An increase in the peptide concentration (> 2mM) was detrimental as expected since an increased of undesired products was determined (e.g. linear and cyclic dimmers).

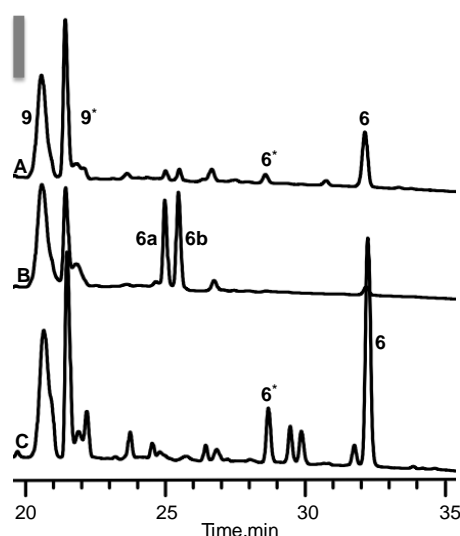


Figure 2. RP-HPLC-UV (210 nm) profiles of T3P-mediated cyclisation of **9** at A) room temperature, B) 0 °C, C) 45 °C; linear gradient of 5%B-95%B over 45 min (ca. 2 %B·min⁻¹), 1 mL·min⁻¹, using XTerra MS C₁₈ column (4.6 mm × 150 mm, 5 µm). A = 0.1% TFA in H₂O and B = 0.1 %TFA ACN. Reaction conditions: 5 equiv. T3P, 6 equiv. DIPEA, DMF/ CH₂Cl₂ (1:1), 1 day. The scale bar shown is equivalent to 300 mUA.

The effect of temperature on cyclisation of **9** with T3P was next studied. When the reaction was carried out for 24 hours at low temperature (0-5 °C), a new set of signals (**6a**, **6b**) were observed by RP-HPLC (Figure 2B) together with **9**, **9*** and a small proportion of **6**. Remarkably, these signals (**6a**, **6b**) presented a mass that corresponded to that of the cyclised product (**6**) (when analyzed by RP-HPLC-UV-ESIMS, see supporting information Figure S26), but exhibited shorter retention times than **6** or **6*** (Figure 2). When the reaction was carried out at 45 °C for 24 hours an increase in the proportion of **6** (53% determined from the RP-HPLC-UV peak area) and **6*** (12%) was observed (relative to the proportions observed when the reaction was carried out at room temperature, 15% and 1% for **6** and **6*** respectively) but **6a**, **6b** were not detected (Figure

2C). It is important to note that species **6a**, **6b** were also detected as minor components of the reaction mixture when the cyclisation was carried out at room temperature (Figure 2A). This indicates that **6a** and **6b** convert into **6** and **6*** respectively.

Therefore, one can conclude that in order to drive the reaction to formation of **6**, this has to be carried out either at room or higher temperatures. This again conflicts with the reported conditions for the synthesis of hirsutide (**2**) but agrees with previous work where cyclisation of activated esters to linear tetrapeptides was carried out at high temperature.

We next monitored the cyclisation of **9** with T3P at 45 °C as a function of time (Figure 3, top). Interestingly, the species **6a**, **6b** appeared at early reaction times, but disappeared during the course of the reaction. Moreover, it is worthy to note that the reaction was not complete using longer reaction times but an increase in **6*** and **9*** together with the appearance of several unidentified impurities was observed (Figure 3). Further experiments showed that when the cyclisation is done at 0-5 °C the species **6a**, **6b** are already present after 1 hour of reaction (Figure 3, bottom), albeit the proportions of **9*** and **6b** are less than **9** and **6a**, relative to when the reaction is carried out for longer times, thus establishing a relationship between these pairs of species.

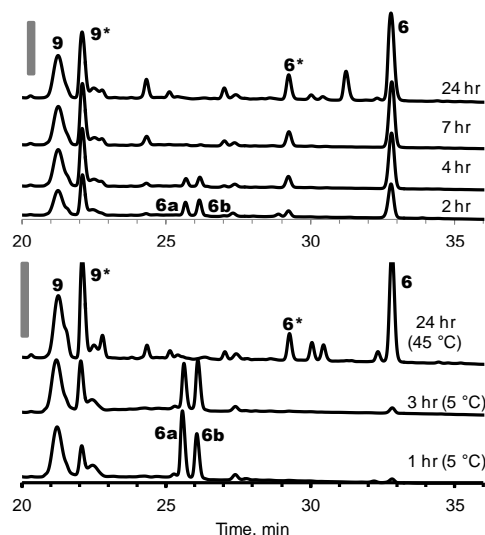


Figure 3. (Top graph) RP-HPLC-UV (210 nm) profiles of T3P-mediated cyclisation of **9** at 45 °C monitored at different times (shown on the right of the HPLC traces). (Bottom graph) RP-HPLC-UV (210 nm) profiles of T3P-mediated cyclisation of **9** at 5 °C for 3 h then 45 °C for 24 h monitored at different times; linear gradient of 5%B-95%B over 45 min (ca. 2 %B·min⁻¹), 1 mL·min⁻¹, using XTerra MS C₁₈ column (4.6 mm × 150 mm, 5 µm). A = 0.1% TFA in H₂O and B = 0.1 %TFA ACN. Reaction conditions: 5 equiv. T3P, 6 equiv. DIPEA, DMF/ CH₂Cl₂ (1:1). The scale bar shown is equivalent to 500 mUA.

To determine if T3P offers an advantage when compared to HBTU or HATU, the synthesis of **6** starting from **9** was carried out with the latter reagents under similar conditions to those using T3P, that is, using 5 equiv. of coupling reagent, 6 equiv. of DIPEA in CH₂Cl₂/DMF (1:1) for 24 hours at room temperature

and at 1 mmol peptide concentration (see supporting information Figure S28). Surprisingly, the reaction with HBTU showed the C-terminal epimerized product **6*** as the main cyclic product of the reaction (~40%, determined from the RP-HPLC-UV peak area), together with a small amount of **6** (~1%) and the *N*-formylated linear peptide (see supporting information Figure S28B). Interestingly, in the reaction with HATU, **6** was not detected but **6a** and **6b** were again observed by RP-HPLC (supporting information Figure S28C). We then performed the reaction with HATU under similar conditions as stated earlier but at 45 °C. This time **6*** was the major product (~70%, determined from the RP-HPLC-UV peak area) and **6** was obtained in lesser amount (~20%) (supporting information Figure S29). These results further highlight the advantage of T3P to maintain stereochemical integrity during the cyclisation step.

We next turned our attention to understand the nature of the species **6a**, **6b** and for this purpose a couple of hypotheses were considered. First, one could argue that **6a**, **6b** correspond to the activated ester linear intermediates of **9**, **9***, if one assumes that **6a**, **6b** are thermally cyclised in the mass spectrometer^[24] but hydrolyzed to **9**, **9*** during chromatography. However, **6a**, **6b** present the same retention times and molecular masses, when using either T3P or HATU as activating agents during the cyclisation of **9**. One would have expected different retention times for the reactive 7-aza-benzotriazol ester of **9** obtained with HATU relative to the carboxylic phosphonic mixed anhydride of **9** obtained with T3P,^[25] which suggests that the hypothesis proposed above is unlikely.

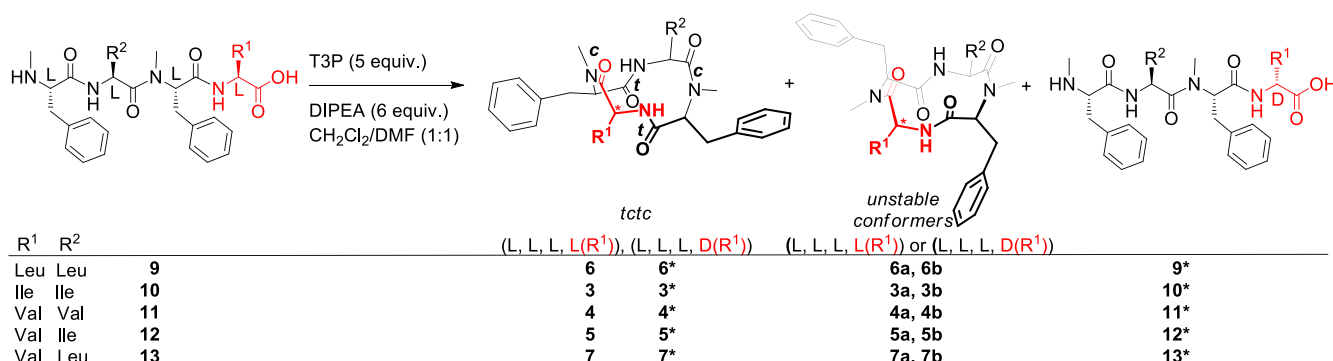
A second explanation for the presence of **6a**, **6b** is to consider these species as less stable cyclic conformers of **6**, **6***. This lower stability can be attributed to a highly constrained conformation. This hypothesis is supported by reports of linear peptides containing *N*-Me-aa which adopt different conformations due to *cis/trans* interconversion and in some cases, such as for peptides containing several *N*-Me-aa, multiple peaks can be seen by reverse-phase RP-HPLC.^[17a, 22] Similar observations have rarely been reported with cyclotetrapeptides containing *N*-Me-aa, an example is the discovery and isolation of

two different conformers of *N*-Me-D-Ala¹-tentoxin analogue of **1** (Figure 1).^[26]

Therefore, based on the evidence presented herein we propose that cyclisation of **9** and **9*** with T3P leads to **6a** and **6b**, respectively. These peptides (**6a** and **6b**) are cyclic unstable kinetic products of the reaction and are conformers of **6** and **6***, respectively, which are the thermodynamic products.

To prove the latter hypothesis we proceeded to identify **6a** and **6b**, by collecting the corresponding fractions *via* preparative RP-HPLC. However, when re-subjecting the purified fractions of **6a** and **6b** to RP-HPLC-UV-ESIMS analysis the retention times and molecular weight of the purified compounds matched those of the linear peptides **9** and **9*** respectively. This indicated that **6a**, **6b**, presumed to be cyclic peptides have been hydrolysed. While the ring opening of cyclotetrapeptides has been reported to occur under relatively mild hydrolytic conditions (Trifluoroacetic acid (TFA)/H₂O, 8:2, 5 hours at temperature),^[14a] there is no precedent for cyclotetrapeptides to undergo ring opening under slightly acidic conditions such as the those used in RP-HPLC (mobile phase consists of 0.1% TFA in H₂O/ACN mixtures). Furthermore, attempts to isolate **6a** and **6b** either by RP-HPLC under neutral conditions or silica gel chromatography failed even when the purification was carried out at low temperatures (e.g. at 5 °C). In both cases only the structures of the linear precursors **9** and **9*** were confirmed after analysis of the attempt to collect fractions corresponding to **6a** and **6b**.

We next proceeded to study the cyclisation reaction by NMR. Therefore, a solution containing **9** at a 2 mM concentration, 1 equiv., of T3P and 2 equiv., of DIPEA in CD₂Cl₂ was prepared. Lowering the amounts of DIPEA and T3P was required to minimize signal overlapping and had no negative effect on the cyclisation reaction. The reaction mixture was kept at 5 °C for 30 min and an aliquot was taken and analyzed by RP-HPLC and by HRMS/MS. The reaction mixture was then inserted into the NMR spectrometer and NMR spectra (¹H and 1D NOE) were acquired at fixed intervals of time while maintaining the reaction temperature at 5 °C for ~30 min, 27 °C for ~1 hr and 45 °C for ~13.3 hr consecutively. Conversion to **6** and **6*** only proceeded at 45 °C in CD₂Cl₂.



Scheme 2. Products observed during the synthesis of cyclotetrapeptides (**3-7**) from their linear precursors (**9-13**).

As expected, the RP-HPLC trace showed the presence of **9** and **6a** as the major species in the reaction mixture and **9*** and **6b** were observed in lower proportion (supporting information Figure S30). The HRMS/MS spectra corresponded to that of a cyclic tetrapeptide (supporting information Figure S31-32). Remarkably, the ^1H NMR spectrum of the reaction mixture at 5 °C, 27 °C and 45 °C did not show traces of the linear peptide **9** (supporting information Figure S33), as evidenced by the absence of the singlet assigned to the *N*-methyl protons of the *N*-terminal HN-Me-Phe^1 , which appears upfield (~ 2.42 ppm) relative to the singlet corresponding to *N*-methyl protons which are part of an amide bond (~ 3.08 - 2.88 ppm) (Figure 4). This result indicates that **6a**, **6b** hydrolysed during the chromatography, and therefore one can conclude that the RP-HPLC traces do not show a true picture on the proportions of **9**, **9*** and **6a**, **6b** in the reaction mixture. The ^1H NMR spectrum of the crude reaction presents several singlets between ~ 3.10 and ~ 2.88 ppm (supporting information Figure S33 and Figure 4), indicating the presence of *N*-methyl protons which are part of an amide bond, thus further confirming a cyclic structure for **6a**, **6b**.

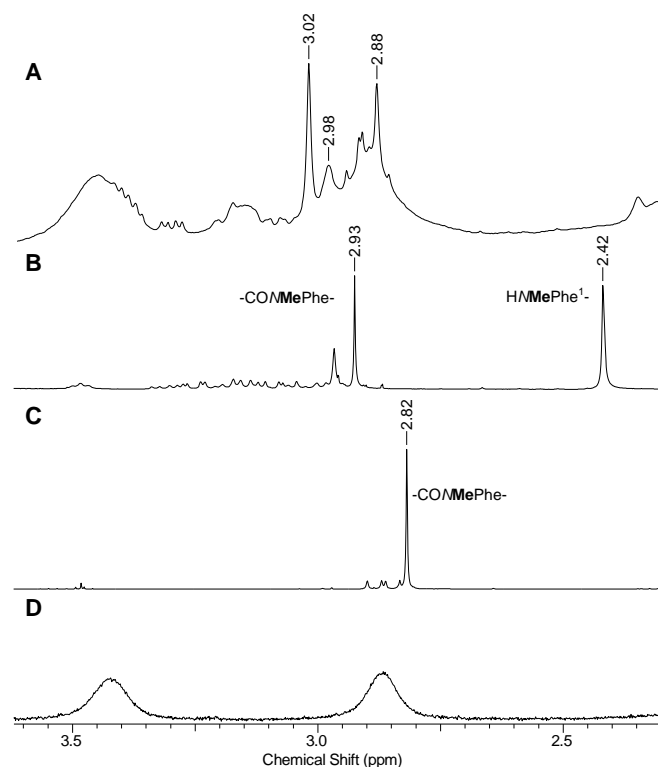


Figure 4. ^1H NMR spectra (500 MHz, CD_2Cl_2 , 27 °C) of A) the reaction mixture of **9** (2 mM), T3P (1 equiv.) and DIPEA (2 equiv.) in CD_2Cl_2 after 30 min. at 5 °C, B) linear peptide **9**, C) cyclic peptide **6** and D) a mixture of T3P and DIPEA (1:2) in CD_2Cl_2 .

Furthermore, the 1D NOE NMR spectra showed a weak NOE correlation between the most intense *N*-methyl protons observed in the ^1H NMR spectra of the reaction mixture (~ 3.02 ppm) (Figure 4A), which based on the RP-HPLC and HRMS/MS spectra corresponds to **6a**, and a signal in the region of the C^αH

protons (~ 4.88 ppm) (supporting information Figure S34). This is indicative of a *trans* configuration for a Leu-*N*-Me-Phe peptide bond.^[22] The 1D NOE spectra also showed that the same *N*-methyl protons (~ 3.02 ppm) are in slow exchange with another set of *N*-methyl protons (~ 2.93 ppm) (supporting information Figure S34). The ^1H NMR spectra of the reaction mixture at 45 °C shows the appearance of three new signals in the *N*-methyl protons region that increase in intensity as the reaction progressed (Figure 5). Two of these signals corresponded with the chemical shift of the isolated peptides **6** and **6***. Also a decrease in the intensity of the signal corresponding to **6a** and a smaller signal was observed. The latter was assigned to **6b**, considering that **6a**, **6b** are the only two cyclic species which are consumed during the reaction and that are observed by RP-HPLC before the reaction mixture was heated to 45 °C. NOE correlations between **6b** and the C^αH protons were not observed and the C^αH protons overlapped strongly, making it difficult to assign correlations among them (supporting information Figure S35).

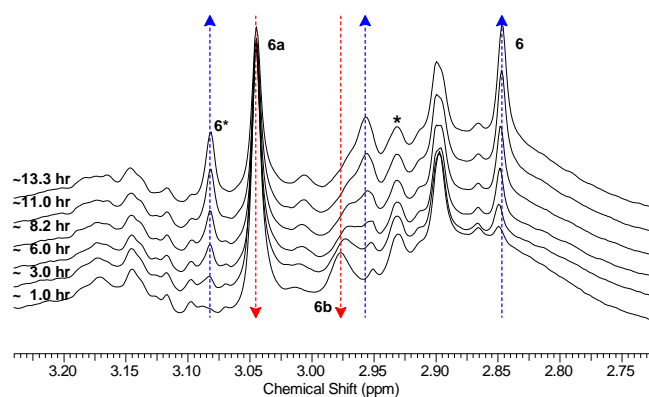
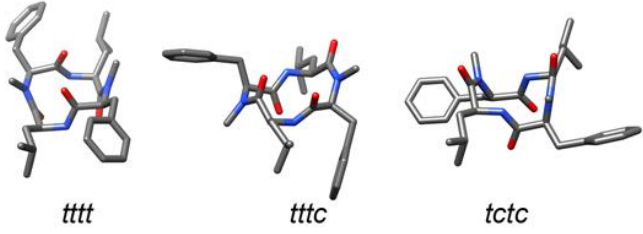


Figure 5. ^1H NMR spectra (500 MHz, CD_2Cl_2 , 45 °C) of the reaction mixture of **9** (2 mM), T3P (1 equiv.) and DIPEA (2 equiv.) in CD_2Cl_2 at different time points. The spectrum shows the *N*-methyl proton region. * indicates the set of *N*-methyl protons which are in exchange with the *N*-methyl protons of **6a**.

In an attempt to elucidate the possible conformations of **6a**, **6b** we performed density functional theory (DFT) calculations and molecular dynamics simulations on three different conformers of **6**: *tctc*, *tttc* and *tttt* (the *cis* conformation was assigned to the Leu-*N*-Me-Phe amide bonds as established by NMR and the all *cis* conformer was omitted from this calculation given the known poor stability of the *cccc* conformer in analogous systems).^[23] The calculations were performed in *vacuum* and in two solvent systems; DMSO and CH_2Cl_2 , which are available in the Gaussian 09^[27] software (DMSO has similar physico-chemical properties to DMF). Our calculations showed that in a solvated system the conformer stability decreases as follows *tctc* > *tttc* > *tttt* (Table 1). However, there is little energy stabilization between the *tttc* and *tttt* conformers in CH_2Cl_2 . The most stable conformer is *tctc* in accord with our experimental results (see Supporting information Figures S22-23). Additionally, the *tttc* conformer displayed a larger dipole moment than *tctc* and *tttt*, which suggests a shorter retention time in reverse phase HPLC

of the former. The *tttt* conformer was more stable than the *tttc* conformer *in vacuo* further highlighting the important role of solvent-peptide interactions on conformer stability. For comparison purposes, we also performed molecular dynamics simulations and subsequent energy calculations using standard molecular mechanics and the GBSA implicit solvent model to simulate the solvent environment in DMF and CH₂Cl₂ for the three conformers of **6**. The potential energy (see supporting information Table S2) calculated for the three conformers exhibited the same trend (*tctc* > *tttc* > *tttt*) as the DFT calculations, which is in agreement with our experimental results, whereby **6a** and **6b** are kinetically controlled products and **6** the thermodynamic product. These theoretical calculations combined with the NMR data indicate that **6a** adopts either a *tttc* or *tttt* unstable conformation (Scheme 2), and these are in slow exchange in solution. Similar conclusions could be drawn after analyzing the DFT calculations for the three different conformers of **6***: *tctc*, *tttc* and *tttt* (see supporting information Table S1).

Table 1. Optimized structures of the different conformers of **6** in a tube representation (top). Potential energy differences relative to the *tctc* conformer (in kcal/mol) and dipole moments (given in parenthesis in Debye) of the three minimised conformers of **6** in *vacuum*, DMSO and CH₂Cl₂.

			
	<i>tttt</i> ($\Delta E^a/\mu^b$)	<i>tttc</i> ($\Delta E/\mu$)	<i>tctc</i> ($\Delta E/\mu$)
Vacuum	8.36/1.00	10.03/4.55	0°/0.21
DMSO	12.64/1.38	11.55/7.19	0°/1.33
CH ₂ Cl ₂	11.74/1.32	11.35/6.60	0°/0.96

[a] ΔE : Potential energy difference (kcal/mol). [b] μ : Dipole moment. [c] The absolute potential energy for *tctc* conformer in *vacuum*, DMSO and CH₂Cl₂ is -1108149.20, -1108162.45 and -1108160.10 kcal/mol, respectively.

With the knowledge gained on the cyclisation of tetrapeptides using T3P we were then able to prepare the cyclotetrapeptide analogue **6** of the onychocins (**3-5**) in acceptable yield while obtaining a small quantity of the C-terminal epimerized product (Table 2) by carrying out the cyclisation in the presence of 5 equiv. of T3P, 6 equiv. DIPEA in CH₂Cl₂/DMF (1:1) for 24 hours at 45° C using 1 mM peptide concentration. This same protocol was then used to synthesize the naturally extracted compounds onychocins (**3-5**, **7**)^[6] starting from the corresponding linear precursors **10-12** and **13**, respectively (Table 2). However, cyclisation yields varied depending on the peptide sequence. To illustrate this point, the peak area of the chromatographic

profiles showing the percent of the various products present in the reaction mixtures for **3-7** at different temperatures are summarized in Table 2. The data clearly indicates a sequence-dependent product distribution. Remarkably, during the synthesis of **7** only the early eluting conformers **7a,7b** were observed at 45 °C. The desired product **7** was obtained in moderate yields when increasing the temperature to 60 °C (Table 2), but also an increase in the proportion of **7*** was observed.

Table 2. The percentage of the various products present during the cyclization of (**9-13**) to cyclic tetrapeptides (**3-7**) determined by RP-HPLC-UV peak (210 nm); linear gradient of 5%B-95%B over 45 min (ca. 2%B/min), 1 mL·min⁻¹, using an XTerra MS C₁₈ column (4.6 mm x 150 mm, 5 μ m). A = 0.1% TFA in H₂O and B = 0.1 %TFA in ACN. Reaction conditions: 5 equiv. T3P, 6 equiv. DIPEA, CH₂Cl₂/DMF (1:1), 1 day.

	3		4		5		6		7		
	rt	45°C	rt	45°C	rt	45°C	rt	45°C	rt	45°C	60°C
CM ^a	3%	36%	19%	50%	10%	36%	15%	53%	-	3%	39%
ECM ^b	-	24%	4%	33%	-	20%	1%	12%	-	4%	22%
OC ^c	28%	-	58%	-	68%	-	3%	-	52%	40%	-
LP ^d	36%	23%	13%	10%	16%	17%	47%	17%	42%	36%	18%
ELP ^e	33%	6%	6%	7%	6%	27%	34%	18%	6%	17%	21%

[a] CM: Cyclic monomer. [b] ECM: epimerised cyclic monomer (**3***, **4***, **5***, **6*** and **7***). [c] OC: other conformers (**3a,3b**, **4a,4b**, **5a,5b**, **6a,6b** and **7a,7b**). [d] LP: linear precursor (**10**, **11**, **12**, **9** and **13**, respectively). [e] ELP: Epimerised linear precursor (**10***, **11***, **12***, **9*** and **13***, respectively).

Finally all the synthetic onychocins reported herein were tested for their antitumor activity. All the cyclotetrapeptides (**3**, **4**, **5**, **6**, and **7**) moderately inhibit the proliferation of mouse myeloma cells in a dose-dependent manner, with IC₅₀ values of 13.8 ± 0.2, 45.5 ± 2.5, 23.1 ± 1.7, 13.2 ± 0.2 and 17.2 ± 0.4 μ g/mL respectively. Notably, there was a decrease in the inhibitory activity with a decrease in the size of the side chains of the amino acids in the cyclotetrapeptide sequence (as exemplified by the IC₅₀ of compounds **4** and **6**). This phenomenon might be indicative of the hydrophobic effect or potential physical and geometric requirements for molecular recognition, which could serve as a lead for further drug development.

Conclusions

The synthesis of the natural onychocins **3-5** and **7** and analogue **6** was successfully accomplished using T3P to effect the key cyclisation step. Nonetheless, there is a need to further explore options to restrict carboxylate epimerization to maximise yields. The cyclisation generates unstable cyclic conformers (kinetic products) that were detected by RP-HPLC-UV-MS and ¹H NMR. The most stable *tctc* conformers are favored using longer reaction times at room temperature or at higher temperatures

and their structures agree with the corresponding natural compounds. Finally, biological evaluation of all the synthetic cyclotetrapeptides revealed moderate antitumor activity.

Experimental Section

Chemistry

General information: All the reagents purchased from commercial sources were reagent grade and were used without further purification. Solvents for peptide synthesis and RP-HPLC were purchased as synthesis grade and HPLC grade, respectively. 2-Chlorotrityl chloride resin and ethyl 2-cyano-(hydroxyimino)acetate (Oxyma) were purchased from Novabiochem (Merck, Germany). O-(Benzotriazol-1-yl)-*N,N,N,N*-tetramethyluronium hexafluorophosphate (HBTU) and 1-hydroxy-7-azabenzotriazole (HOAt) were acquired from GL Biochem (Shanghai, China), while O-(7-azabenzotriazol-1-yl)-*N,N,N,N*-tetramethyluronium hexafluorophosphate (HATU) and 6-chloro-1-hydroxybenzotriazole (6-Cl-HOBT) were purchased from Chempep (Wellington, USA) and Aapptec (Louisville, USA), respectively. Collidine, pyridine, piperidine, 2-propanephosphonic acid anhydride (T3P) solution (50% in ethyl acetate), 2,2,2-trifluoroethanol (TFE), *N,N*-diisopropylethylamine (iPr₂NEt) and *N,N*-diisopropylcarbodiimide (DIC) were purchased from Sigma-Aldrich (St. Louis, USA). *N,N*-Dimethyl-4-aminopyridine (DMAP) and 1,1,1,3,3,3-hexafluoropropan-2-ol (HFIP) were purchased from AK Scientific (Union City, USA). Dimethylformamide (DMF, AR grade), acetonitrile (CH₃CN, HPLC grade) and trifluoroacetic acid (TFA) were purchased from Scharlau (Barcelona, Spain). Dichloromethane (AR grade) was obtained from ECP Limited (Auckland, New Zealand). All the Fmoc-amino acids (Fmoc-Leu-OH, Fmoc-Ile-OH and Fmoc-Val-OH) were purchased from GL Biochem except Fmoc-*N*-Me-Phe-OH which was purchased from Aapptec.

Infrared spectra were recorded on a Perkin Elmer Spectrum 100 infrared spectrometer, each spectrum was collected with 64 scans at a resolution of 4 cm⁻¹. Optical rotations were determined at the sodium D line (589 nm) at 23 °C using a Perkin Elmer 341 instrument. ¹H, ¹³C and 1D NOE nuclear magnetic resonance experiments were performed on a Bruker AVANCE 400 (¹H 400 MHz; ¹³C 100 MHz) or 500 (¹H 500 MHz; ¹³C 125 MHz) spectrometer in deuterated MeOH, CHCl₃, CH₂Cl₂ or DMSO. Chemical shifts were recorded in parts per million (ppm) and were referenced to the residual MeOH signal at 3.31 ppm or the tetramethylsilane signal at 0.00 ppm. The ¹³C values were also presented relative to the signal of residual MeOH or chloroform at 49.0 ppm or 77.0 ppm, respectively. ¹H NMR spectral data were reported as follows: chemical shift (δ_{H}), relative integral, multiplicity (s, singlet; d, doublet; t, triplet; q, quartet; m, multiplet; dd, doublet of doublets; dq, doublet of quartets; ddd, doublet of doublet of doublets) and coupling constant (*J* in Hz). The 1D NOE were done with 1 sec mixing time. High-resolution mass spectra were obtained on a Bruker micrOTOFQ mass spectrometer using electrospray ionization (ESI) under positive mode. All the analytical RP-HPLC experiments were carried out using an analytical column (XTerra MS C₁₈, 125 Å, 4.6 mm × 150 mm, 5 µm) on a Dionex Ultimate 3000 System with a 45 min linear gradient of 5-95% solvent B (where solvent A was 0.1% TFA in water and solvent B was 0.1% TFA in acetonitrile) at a flow rate of 1 mL·min⁻¹ and UV signals were detected at the wavelengths 210, 225, 254 and 280 nm. Semi-preparative RP-HPLC was carried out on a Waters 600 system using a semi-preparative column (XTerra MS C₁₈ Prep Column, 125 Å, 19 mm × 300 mm, 10 µm) at a flow rate of 10 mL·min⁻¹ using a adjusted gradient of 5-95% solvent B according to the elution profiles obtained from analytical RP-HPLC chromatography. RP-HPLC-UV-ESIMS analysis was conducted on either

an Agilent Technologies 1120 Compact LC equipped with a Hewlett-Packard 1100 MSD mass spectrometer or an Agilent Technologies 1260 Infinity LC equipped with an Agilent Technologies 6120 Quadrupole mass spectrometer using an analytical column (GraceSmart C₁₈, 120 Å, 4.6 × 150 mm 5 µm) with a 30 min linear gradient of 5-95% solvent B at a flow rate of 0.3 mL·min⁻¹. Thin layer chromatography (TLC) was performed using F254 0.2 mm silica plates, followed by visualization with UV irradiation at 254 nm. Flash column chromatography was performed using 63–100 µm silica gel.

Synthesis of linear peptides

All the linear peptides were prepared on 2-chlorotrityl chloride resin on a 0.1 mmol scale using the Fmoc-SPPS strategy.

H-Leu-MMePhe-Leu-MMePhe-OH (8): A solution of Fmoc-MMePhe-OH (80 mg, 0.2 mmol) and DIPEA (64.5mg, 0.5 mmol) in CH₂Cl₂ (3 mL) was added to the pre-swollen 2-chlorotrityl chloride resin (in CH₂Cl₂), and the resulting mixture was agitated at rt for 1 h. The resin was then treated with a mixture of CH₂Cl₂:MeOH:DIPEA (16:3:1, 3 mL, 2 × 15 min) in order to cap the resin unreacted active sites. Fmoc deprotection was achieved by using 20% piperidine in DMF (5 mL, 2 × 10 min), followed by amino acid coupling. The two Leu residues were coupled to the sequence by treating the resin with a solution of Fmoc-Leu-OH (282 mg, 0.8 mmol), HATU (300 mg, 7.9 mmol) and DIPEA (206 mg, 1.6 mmol) in 5 mL of DMF at rt for 2h and double couplings were performed. The coupling of *N*-Me-Phe was accomplished using a mixture of Fmoc-*N*-MePhe-OH (160 mg, 0.4 mmol), HATU (148 mg, 3.9 mmol) and DIPEA (103 mg, 0.8 mmol) in 3 mL of DMF at rt for 45 min. After chain elongation, the linear peptide was cleaved from the resin by treatment with HFIP: CH₂Cl₂ (1:4, 5 mL) at rt for 1h. The resin was filtered and washed with CH₂Cl₂ (2 × 1 mL). The resulting filtrates were combined, followed by removal of solvent and volatile HFIP under a dry nitrogen flow. Finally the crude reaction mixture was re-dissolved in 50% acetonitrile aqueous solution, lyophilized and purified by semi-preparative RP-HPLC to quantitatively afford **8** as a white powder. Anal. RP-HPLC: *t*_R = 18.28 min (GraceSmart C₁₈, 120 Å, 4.6 × 150 mm, 5 µm, 5% B to 95% B at 3% B per min, 0.3 mL·min⁻¹). MS (ESI+): C₃₂H₄₆N₄O₅ [M+H]⁺ calcd./found 567.3/567.4.

H-MMePhe-Leu-MMePhe-Leu-OH (9): The preparation of **9** was conducted using a similar procedure to that described above for the synthesis of **8**. Anal. RP-HPLC: *t*_R = 21.2 min (GraceSmart C₁₈, 120 Å, 4.6 × 150 mm, 5 µm, 5% B to 95% B at 3% B per min, 0.3 mL·min⁻¹). MS (ESI+): C₃₂H₄₆N₄O₅ [M+H]⁺ calcd./found 567.3/567.4.

H-MMePhe-Leu-MMePhe-D-Leu-OH (9*): The preparation of **9*** was conducted using a similar procedure to that described above for the synthesis of **8**. Anal. RP-HPLC: *t*_R = 22.53 min (GraceSmart C₁₈, 120 Å, 4.6 × 150 mm, 5 µm, 5% B to 95% B at 3% B per min, 0.3 mL·min⁻¹). MS (ESI+): C₃₂H₄₆N₄O₅ [M+H]⁺ calcd./found 567.3/567.4.

H-MMePhe-Ile-MMePhe-Ile-OH (10): The preparation of **10** was conducted using a similar procedure to that described above for the synthesis of **8**. Anal. RP-HPLC: *t*_R = 22.9 min (GraceSmart C₁₈, 120 Å, 4.6 × 150 mm, 5 µm, 5% B to 95% B at 3% B per min, 0.3 mL·min⁻¹). MS (ESI+): C₃₂H₄₆N₄O₅ [M+H]⁺ calcd./found 567.3/567.4.

H-MMePhe-Val-MMePhe-Val-OH (11): The preparation of **11** was performed using a similar procedure to that described above for the synthesis of **8**. Anal. RP-HPLC: *t*_R = 20.1 min (GraceSmart C₁₈, 120 Å, 4.6 × 150 mm, 5 µm, 5% B to 95% B at 3% B per min, 0.3 mL·min⁻¹). MS (ESI+): C₃₀H₄₂N₄O₅ [M+H]⁺ calcd./found 539.3/539.3.

H-MMePhe-Ile-MMePhe-Val-OH (12): The preparation of **12** was performed using a similar procedure to that described above for the synthesis of **8**. Anal. RP-HPLC: t_R = 20.8 min (GraceSmart C₁₈, 120 Å, 4.6 x 150 mm, 5 µm, 5% B to 95% B at 3% B per min, 0.3 mL·min⁻¹). MS (ESI+): C₃₁H₄₄N₄O₅ [M+H]⁺ calcd./found 553.2/553.4.

H-MMePhe-Leu-MMePhe-Val-OH (13): The preparation of **13** was performed using a similar procedure to that described above for the synthesis of **8**. Anal. RP-HPLC: t_R = 22.0 min (GraceSmart C₁₈, 120 Å, 4.6 x 150 mm, 5 µm, 5% B to 95% B at 3% B per min, 0.3 mL·min⁻¹). MS (ESI+): C₃₁H₄₄N₄O₅ [M+H]⁺ calcd./found 553.2/553.4.

Synthesis of cyclotetrapeptides

Cyclo[Leu-MMePhe-Leu-MMePhe] (6): To a solution of **9** (17.1 mg, 30.2 µmol) and T3P (90 µL, 151.0 µmol) in CH₂Cl₂:DMF (1:1, 30 mL) was added DIPEA (31.6 µL, 181.2 µmol) and the reaction mixture was stirred at 45 °C for 1 day. After evaporation of CH₂Cl₂ under reduced pressure, the reaction residue was purified by semi-preparative RP-HPLC to give **6** as a colorless powder (8.8 mg, 53%). Anal. RP-HPLC: t_R = 31.6 min (XTerra MS C₁₈, 125 Å, 4.6 mm x 150 mm, 5 µm, 5% B to 95% B at 2% B per min, 1 mL·min⁻¹); [α]_D^{23.2} -218.75 (c 0.08, CH₂Cl₂); IR (cm⁻¹): 3317, 3064, 3027, 2956, 2927, 2870, 1655, 1629, 1498, 1454, 1402, 1323, 1300, 1172, 1090, 965, 731, 700. ¹H NMR (400 MHz, CDCl₃): δ = 7.31 (t, J =7.4, 4 H, CH_{Ar}), 7.24 (d, J =7.2, 6 H, CH_{Ar}), 6.99 (d, J =9.2, 2 H, 2 x CONH), 4.61 (m, 4 H, 2 x α-CH (Leu) and 2 x α-CH (MMePhe)), 3.77 (d, J =13.9, 2 H, 2 x β-CH_{2a} (MMePhe)), 2.89 (d, J =12.0, 2 H, 2 x β-CH_{2b} (MMePhe)), 2.83 (s, 6 H, 2 x N-CH₃), 1.66 (m, 2 H, 2 x β-CH_{2a} (Leu)), 1.40 (m, 2 H, 2 x γ-CH (Leu)), 1.29 (d, J =6.0, 2 H, 2 x β-CH_{2b} (Leu)), 0.84 (d, J =6.5, 6 H, 2 x CHCH₃), 0.78 (d, J =6.6, 6 H, CHCH₃) ppm. ¹³C NMR (100 MHz, CDCl₃): δ = 173.4 (C=O (MMePhe)), 170.1 (C=O (Leu)), 137.4 (C_{Ar}), 129.6 (CH_{Ar}), 128.6 (CH_{Ar}), 127.7 (CH_{Ar}), 63.8 (α-CH (MMePhe)), 49.2 (α-CH (Leu)), 41.4 (β-CH₂ (Leu)), 34.9 (β-CH₂ (MMePhe)), 31.0 (N-CH₃), 25.2 (γ-CH (Leu)), 22.9 (CHCH₃), 22.8 (CHCH₃) ppm; HRMS (ESI+): C₃₂H₄₄N₄O₄Na [M+Na]⁺ calcd./found 571.3255/571.3259.

Cyclo[Ile-MMePhe-Ile-MMePhe] (3): **3** was obtained as a colorless powder (7.7 mg, 36%) from its linear precursor **10** (22.1 mg, 39.0 µmol) using a similar method to that described for **6**. Anal. RP-HPLC: t_R = 31.6 min (XTerra MS C₁₈, 125 Å, 4.6 mm x 150 mm, 5 µm, 5% B to 95% B at 2% B per min, 1 mL·min⁻¹); [α]_D^{23.2} -153.00 (c 0.1, CH₂Cl₂); IR (cm⁻¹): 3328, 3065, 3032, 2967, 2933, 2877, 1652, 1628, 1498, 1455, 1405, 1321, 1298, 1168, 1089, 973, 738, 700; δ = ¹H NMR (400 MHz, MeOD): δ = 7.32 (m, 10 H, CH_{Ar}), 4.51 (m, 2 H, 2 x α-CH (Ile)), 4.32 (t, J =8.7, 2 H, 2 x α-CH (MMePhe)), 3.69 (d, J =13.3, 2 H, 2 x β-CH_{2a} (MMePhe)), 3.03 (m, 2 H, 2 x β-CH_{2b} (MMePhe)), 2.88 (s, 6 H, 2 x N-CH₃), 1.87 (m, 2 H, 2 x β-CH (Ile)), 1.52 (dd, J =12.7, 7.7, 2 H, 2 x γ-CH_{2a} (Ile)), 1.02 (dt, J =16.2, 6.9, 2 H, 2 x γ-CH_{2b} (Ile)), 0.90 (t, J =7.3, 6 H, 2 x CH₂CH₃), 0.72 (d, J =6.3, 6 H, 2 x CHCH₃) ppm. ¹³C NMR (100 MHz, MeOD): δ = 173.5 (C=O (Ile)), 172.2 (C=O (MMePhe)), 138.8 (C_{Ar}), 130.1 (CH_{Ar}), 129.7 (CH_{Ar}), 128.3 (CH_{Ar}), 64.6 (α-CH (MMePhe)), 56.8 (α-CH (Ile)), 37.0 (β-CH (Ile)), 35.1 (β-CH₂ (MMePhe)), 31.5 (N-CH₃), 25.6 (γ-CH₂ (Ile)), 17.2 (CHCH₃), 12.0 (CH₂CH₃) ppm; HRMS (ESI+): C₃₂H₄₅N₄O₄ [M+H]⁺ calcd./found 549.3363/549.3425.

Cyclo[Val-MMePhe-Val-MMePhe] (4): **4** was obtained as a colorless powder (12.2 mg, 50%) from its linear precursor **11** (25.3 mg, 47.0 µmol) using a similar method to that described for **6**. Anal. RP-HPLC: t_R = 28.9 min (XTerra MS C₁₈, 125 Å, 4.6 mm x 150 mm, 5 µm, 5% B to 95% B at 2% B per min, 1 mL·min⁻¹); [α]_D^{23.2} -205.25 (c 0.08, CH₂Cl₂); IR (cm⁻¹): 3323, 3065, 3031, 2966, 2931, 2875, 1662, 1629, 1497, 1454, 1404, 1386, 1172, 1089, 978, 733, 699; ¹H NMR (400 MHz, MeOD) δ = 7.32 (m, 10 H, CH_{Ar}), 4.50 (dd, J =11.5, 3.0, 2 H, 2 x α-CH (MMePhe)), 4.24 (d,

J =8.1, 2 H, 2 x α-CH (Val)), 3.69 (d, J =12.1, 2 H, 2 x β-CH_{2a} (MMePhe)), 3.03 (dd, J =15.1, 11.3, 2 H, 2 x β-CH_{2b} (MMePhe)), 2.87 (s, 6 H, 2 x N-CH₃), 2.13 (dd, J =14.1, 6.9, 2 H, 2 x β-CH (Val)), 0.89 (d, J =6.8, 6 H, 2 x CHCH₃), 0.74 (d, J =6.4, 6 H, 2 x CHCH₃). ¹³C NMR (100 MHz, MeOD): δ = 173.3 (C=O (Val)), 172.1 (C=O (MMePhe)), 138.7 (C_{Ar}), 130.0 (CH_{Ar}), 129.5 (CH_{Ar}), 128.1 (CH_{Ar}), 64.6 (α-CH (MMePhe)), 57.3 (α-CH (Val)), 35.2 (β-CH₂ (MMePhe)), 31.2 (N-CH₃), 20.9 (CHCH₃), 18.5 (CHCH₃) ppm; HRMS (ESI+): C₃₀H₄₀N₄O₄Na [M+Na]⁺ calcd./found 543.3050/543.2951.

Cyclo[Ile-MMePhe-Val-MMePhe] (5): **5** was obtained as a colorless powder (6.1 mg, 36%) from its linear precursor **12** (18.1 mg, 32.8 µmol) using a similar method to that described for **6**. Anal. RP-HPLC: t_R = 30.2 min (XTerra MS C₁₈, 125 Å, 4.6 mm x 150 mm, 5 µm, 5% B to 95% B at 2% B per min, 1 mL·min⁻¹); [α]_D^{23.2} -149.23 (c 0.1, CH₂Cl₂); IR (cm⁻¹): 3323, 3065, 3031, 2967, 2933, 2877, 1657, 1630, 1498, 1455, 1404, 1386, 1320, 1169, 1089, 975, 737, 700; ¹H NMR (400 MHz, MeOD) δ = 7.31 (m, 10 H, CH_{Ar}), 4.50 (m, 2 H, 2 x α-CH (MMePhe)), 4.31 (t, J =7.5, 1 H, α-CH (Ile)), 4.25 (t, J =7.5, 1 H, α-CH (Val)), 3.63 (d, 14.9, 2 H, 2 x β-CH_{2a} (MMePhe)), 3.02 (dd, J =14.9, 11.5, 2 H, 2 x β-CH_{2b} (MMePhe)), 2.87 (s, 3 H, N-CH₃), 2.86 (s, 3 H, N-CH₃), 2.12 (dd, J =14.0, 7.0, 1 H, β-CH (Val)), 1.86 (m, 1 H, β-CH (Ile)), 1.50 (m, 1 H, γ-CH_{2a} (Ile)), 1.01 (m, 1 H, γ-CH_{2b} (Ile)), 0.89 (t, J =6.4, 6 H, CH₂CH₃ (Ile) and CHCH₃ (Val)), 0.72 (dd, J =12.4, 6.4, 6 H, CHCH₃ (Val) and CHCH₃ (Ile)) ppm. ¹³C NMR (125 MHz, MeOD): δ = 173.6 (C=O (Val) and C=O (Ile)), 172.1 (C=O (MMePhe)), 139.0 (C_{Ar}), 130.1 (CH_{Ar}), 129.7 (CH_{Ar}), 128.3 (CH_{Ar}), 64.7 (α-CH (MMePhe)), 57.5 (α-CH (Val)), 56.7 (α-CH (Ile)), 36.9 (β-CH₂ (Ile)), 35.3 (β-CH₂ (MMePhe)), 31.4 (N-CH₃), 30.4 (β-CH (Val)), 25.8 (γ-CH₂ (Ile)), 20.9 (CHCH₃ (Val)), 18.7 (CHCH₃ (Val)), 17.2 (CHCH₃ (Ile)), 12.1 (CH₂CH₃) ppm; HRMS (ESI+): C₃₁H₄₂N₄O₄Na [M+Na]⁺ calcd./found 557.3206/557.3089.

Cyclo[Leu-MMePhe-Val-MMePhe] (7): **7** was obtained as a colorless powder (8.8 mg, 40%) from its linear precursor **13** (22.7 mg, 41.1 µmol) using a similar method to that described for **6** but the reaction was carried out at 60 °C. Anal. RP-HPLC: t_R = 30.4 min (XTerra MS C₁₈, 125 Å, 4.6 mm x 150 mm, 5 µm, 5% B to 95% B at 2% B per min, 1 mL·min⁻¹); [α]_D^{23.2} -173.00 (c 0.2, CH₂Cl₂); IR (cm⁻¹): 3323, 3063, 3031, 2961, 2928, 2872, 1654, 1626, 1498, 1455, 1403, 1387, 1322, 1167, 1089, 975, 731, 700; ¹H NMR (400 MHz, CDCl₃) δ = 7.23 (m, 10 H, CH_{Ar}), 6.89 (t, 8.5, 2 H, CONH (Leu) and CONH (Val)), 4.59 (m, 3 H, 2 x α-CH (MMePhe) and α-CH (Leu)), 4.23 (t, 8.9, 1 H α-CH (Val)), 3.77 (t, 13.6, 2 H, 2 x β-CH_{2a} (MMePhe)), 2.90 (m, 2 H, 2 x β-CH_{2b} (MMePhe)), 2.85 (s, 3 H, N-CH₃), 2.81 (s, 3 H, N-CH₃), 2.08 (m, 1 H, β-CH (Val)), 1.66 (m, 2 H, 2 x β-CH_{2a} (Leu)), 1.39 (m, 2 H, 2 x γ-CH (Leu)), 1.25 (m, 2 H, 2 x β-CH_{2b} (Leu)), 0.84 (t, J =6.7, 3 H, CHCH₃), 0.77 (d, J =6.6, 3 H, CHCH₃) ppm. ¹³C NMR (100 MHz, CDCl₃): δ = 173.2 (C=O (Val)), 172.5 (C=O (MMePhe)), 169.8 (C=O (Leu)), 137.1 (C_{Ar}), 129.2 (CH_{Ar}), 128.4 (CH_{Ar}), 127.4 (CH_{Ar}), 63.6 (α-CH (MMePhe)), 63.2 (α-CH (MMePhe)), 56.2 (α-CH (Val)), 49.0 (α-CH (Leu)), 41.0 (β-CH₂ (Leu)), 34.8 (β-CH₂ (MMePhe)), 31.0 (N-CH₃), 29.3 (β-CH (Val)), 24.7 (γ-CH (Leu)), 22.7 (CHCH₃ (Leu)), 22.5 (CHCH₃ (Leu)), 22.2 (CHCH₃ (Val)), 18.3 (CHCH₃ (Val)) ppm; HRMS (ESI+): C₃₁H₄₂N₄O₄Na [M+Na]⁺ calcd./found 557.3206/557.3206.

Molecular modeling

The structures of three different conformers were built in Discovery Studio 3.0 (DS) using the Charmm Forcefield.^[28] The geometry optimizations and energy calculations of the resulting structures were then carried out in Gaussian 09 at the B3LYP/6-31G(d,p) level with standard settings. Solvation in CH₂Cl₂ and DMSO was modelled by a polarizable continuum model. For comparison, the three backbone conformers were also submitted to a constrained molecular dynamics simulation at a time step of 1 fs. The constraints included only the

dihedral angle of the two methylated amide bonds with values set as 0° or 180° referring to *cis* and *trans* conformations respectively, and the constant force was set to 0.05 kcal/mol·deg. The detailed procedures of molecular dynamics are summarized as follows: Minimised structure was heated to 300 K for 20 ps, followed by 100 ps equilibration at the same temperature. The production phase was performed for 10 ns with samples taken at an interval of 1 ps. The final energy minimisation of the resulting conformations from MD was achieved by 1000 steps of steepest descent followed by another 500 steps of conjugate gradient minimisation. The GBSA implicit solvent model using the dielectric constant of DMF (38) and CH₂Cl₂ (9) was applied for simulations in DMF and CH₂Cl₂.

Bioassays

The peptides were dissolved in DMSO to provide 10 mg/mL stock solutions. An aliquot of each stock solution was transferred to the first lane of Rows B to G in a 96-well microtitre plate and two-fold serially diluted across the 12 lanes of the plate to provide a 2,048-fold concentration gradient. Bioassay medium was added to an aliquot of each test solution to provide a 100-fold dilution into the final bioassay, thus yielding a test range of 100 to 0.05 g/mL. Row A was used as the positive control (no inhibition) and Row H was used as the negative control (complete inhibition). CyTOX is an indicative bioassay platform for discovery of antitumour actives. NS-1 (ATCC TIB-18) mouse myeloma cells were inoculated in 96-well microtitre plates (190 L) at 50,000 cells/mL in DMEM (Dulbecco's Modified Eagle Medium + 10% fetal bovine serum (FBS) + 1% penicillin/streptomycin (Life Technologies)) and incubated in 37 °C (5% CO₂) incubator. At 48 h, resazurin (120 g/mL; 10 L) was added to each well and the plates were incubated for a further 48 h. Finally, the absorbance of each well at 605 nm was measured using a Spectromax plate reader (Molecular Devices).

Acknowledgements

We sincerely thank Mr Daniel Vuong (MST) for performing the bioassay and Mr. Yi Zou from China Pharmaceutical University for providing access to the Gaussian 09 and Discovery Studio 3.0 software packages. The authors would also like to thank the China Scholarship Council (S.Z.) and the Australian Research Council (FT130100142; A.P.) for financial support.

Keywords: cyclisation • tetrapeptides • conformational analysis • natural products • biological activity

- [1] W. L. Meyer, L. F. Kuyper, D. W. Phelps, A. W. Cordes, *J. Chem. Soc. Chem. Comm.* **1974**, 339-340.
- [2] E. L. Kim, J. L. Li, B. Xiao, J. Hong, E. S. Yoo, W. D. Yoon, J. H. Jung, *Chem. Pharm. Bull.* **2012**, 60, 1590-1593.
- [3] a) H. A. Lim, C. Kang, C. S. B. Chia, *Int. J. Pept. Res. Ther.* **2010**, 16, 145-152; b) L. L. Ling, T. Schneider, A. J. Peoples, A. L. Spoering, I. Engels, B. P. Conlon, A. Mueller, T. F. Schäberle, D. E. Hughes, S. Epstein, M. Jones, L. Lazarides, V. A. Steadman, D. R. Cohen, C. R. Felix, K. A. Fetterman, W. P. Millett, A. G. Nitti, A. M. Zullo, C. Chen, K. Lewis, *Nature* **2015**, 517, 455-459.
- [4] a) Y. Nakao, S. Yoshida, S. Matsunaga, N. Shindoh, Y. Terada, K. Nagai, J. K. Yamashita, A. Ganesan, R. W. M. Van Soest, N. Fusetani, *Angew. Chem. Int. Ed.* **2006**, 45, 7553-7557; b) D. M. Hutt, C. A. Olsen, C. J. Vickers, D. Herman, M. A. Chalfant, A. Montero, L. J. Leman, R. Burkle, B. E. Maryanoff, W. E. Balch, M. R. Ghadiri, *ACS Med. Chem. Lett.* **2011**, 2, 703-707; c) M. P. I. Bhuiyan, T. Kato, T. Okauchi, N. Nishino, S. Maeda, T. G. Nishino, M. Yoshida, *Bioorg. Med. Chem.* **2006**, 14, 3438-3446; dS. Mei, A. D. Ho, U. Mahlknecht, *Int. J. Oncol.* **2004**, 25, 1509-1519.
- [5] Y. Terui, Y. w. Chu, J. y. Li, T. Ando, T. Fukunaga, T. Aoki, Y. Toda, *Bioorg. Med. Chem. Lett.* **2008**, 18, 6321-6323.
- [6] I. Pérez-Victoria, J. Martín, V. González-Menéndez, N. de Pedro, N. El Aouad, F. J. Ortiz-López, J. R. Tormo, G. Platas, F. Vicente, G. F. Bills, O. Genilloud, M. A. Goetz, F. Reyes, *J. Nat. Prod.* **2012**, 75, 1210-1214.
- [7] W. L. Meyer, G. E. Templeton, C. I. Grable, C. W. Sigel, R. Jones, S. H. Woodhead, C. Sauer, *Tetrahedron Lett.* **1971**, 12, 2357-2360.
- [8] G. Lang, J. W. Blunt, N. J. Cummings, A. L. J. Cole, M. H. G. Munro, *J. Nat. Prod.* **2005**, 68, 1303-1305.
- [9] C. Almeida, F. El Maddah, S. Kehraus, G. Schnakenburg, G. M. König, *Org. Lett.* **2016**, 18, 528-531.
- [10] H. Guo, N. B. Kreuzenbeck, S. Otani, M. Garcia-Altares, H. M. Dahse, C. Weigel, D. K. Aanen, C. Hertweck, M. Poulsen, C. Beemelmans, *Org. Lett.* **2016**, 18, 3338-3341.
- [11] H. Kawagishi, A. Somoto, J. Kuranari, A. Kimura, S. Chiba, *Tetrahedron Lett.* **1993**, 34, 3439-3440.
- [12] a) D. A. Horton, G. T. Bourne, J. Coughlan, S. M. Kaiser, C. M. Jacobs, A. Jones, A. Ruhmann, J. Y. Turner, M. L. Smythe, *Organic & Biomolecular Chemistry* **2008**, 6, 1386-1395; b) K. A. Fairweather, N. Sayyadi, I. J. Luck, J. K. Clegg, K. A. Jolliffe, *Org. Lett.* **2010**, 12, 3136-3139.
- [13] L. M. De Leon Rodriguez, A. J. Weidkamp, M. A. Brimble, *Org. Biomol. Chem.* **2015**, 13, 6906-6921.
- [14] a) W. Mastle, U. Link, W. Witschel, U. Thewalt, T. Weber, M. Rothe, *Biopolymers* **1991**, 31, 735-744; b) J. Pastuszak, J. H. Gardner, J. Singh, D. H. Rich, *J. Org. Chem.* **1982**, 47, 2982-2987.
- [15] C. A. Lipinski, F. Lombardo, B. W. Dominy, P. J. Feeney, *Adv. Drug Deliv. Rev.* **1997**, 23, 3-25.
- [16] M. J. O. Anteunis, C. Van Der Auwera, *Int. J. Pept. Prot. Res.* **1988**, 31, 301-310.
- [17] aM. Teixidó, F. Albericio, E. Giralt, *J. Pept. Res.* **2005**, 65, 153-166; bR. Roodbeen, S. L. Pedersen, M. Hosseini, K. J. Jensen, *Eur. J. Org. Chem.* **2012**, 7106-7111.
- [18] a) K. Titlestad, *Acta Chem Scand B* **1977**, 31, 523-526; b) S. A. Miller, S. L. Griffiths, D. Seebach, *Helv. Chim. Acta* **1993**, 76, 563-595; c) D. Seebach, O. Bezençon, B. Jaun, T. Pietzonka, J. L. Matthews, F. N. M. Kühnle, W. B. Schweizer, *Helv. Chim. Acta* **1996**, 79, 588-608.
- [19] a) D. H. Rich, P. Mathiaraman, *Tetrahedron Lett.* **1974**, 15, 4037-4040; b) D. H. Rich, P. Bhatnagar, P. Mathiaraman, J. A. Grant, J. P. Tam, *J. Org. Chem.* **1978**, 43, 296-302; c) J. V. Edwards, A. R. Lax, E. B. Lillehoj, G. J. Boudreaux, *Int. J. Pept. Prot. Res.* **1986**, 28, 603-612; d) F. Cavellier, J. Verducci, *Tetrahedron Lett.* **1995**, 36, 4425-4428; e) N. Loiseau, F. Cavellier, J. P. Noel, J. M. Gomis, *J. Pept. Sci.* **2002**, 8, 335-346.
- [20] R. Dahiya, M. Maheshwari, A. Kumar, *Monatsh. Chem.* **2009**, 140, 121-127.

-
- [21] aJ. Klose, M. Bienert, C. Mollenkopf, D. Wehle, C. W. Zhang, L. A. Carpino, P. Henklein, *Chem. Commun.* **1999**, 1847-1848; bJ. R. Dunetz, Y. Xiang, A. Baldwin, J. Ringling, *Org. Lett.* **2011**, 13, 5048-5051.
- [22] D. Sýkora, L. Žáková, M. Buděšínský, *J. Chromatogr. A* **2007**, 1160, 128-136.
- [23] Y. Che, G. R. Marshall, *J. Med. Chem.* **2006**, 49, 111-124.
- [24] X. Yan, R. M. Bain, R. G. Cooks, *Angew. Chem. Int. Ed.* **2016**.
- [25] E. Valeur, M. Bradley, *Chem. Soc. Rev.* **2009**, 38, 606-631.
- [26] D. H. Rich, P. K. Bhatnagar, *J. Am. Chem. Soc.* **1978**, 100, 2218-2224.
- [27] *Gaussian 09, Revision B.09, Gaussian Inc., Wallingford CT, 2009.*
- [28] B. R. Brooks, R. E. Brucoleri, B. D. Olafson, D. J. States, S. Swaminathan, M. Karplus, *J. Comput. Chem.* **1983**, 4, 187-217.
-

Table of contents

Figure S1. Analytical RP-HPLC profile of cyclo[Ile- <i>N</i> MePhe-Ile- <i>N</i> MePhe] (3)	S4
Figure.S2. HRMS profile of synthetic cyclo[Ile- <i>N</i> MePhe-Ile- <i>N</i> MePhe] (3)	S4
Figure.S3. ¹ H NMR spectrum (400 MHz, CD ₃ OD) of cyclo[Ile- <i>N</i> MePhe-Ile- <i>N</i> MePhe] (3)	S5
Figure.S4. ¹³ C NMR spectrum (100 MHz, CD ₃ OD) of cyclo[Ile- <i>N</i> MePhe-Ile- <i>N</i> MePhe] (3)	S5
Figure.S5. IR spectrum of cyclo[Ile- <i>N</i> MePhe-Ile- <i>N</i> MePhe] (3)	S6
Figure S6. Analytical RP-HPLC profile of cyclo[Val- <i>N</i> MePhe-Val- <i>N</i> MePhe] (4)	S6
Figure S7. HRMS profile of synthetic cyclo[Val- <i>N</i> MePhe-Val- <i>N</i> MePhe] (4)	S7
Figure S8. ¹ H NMR spectrum (400 MHz, CD ₃ OD) of cyclo[Val- <i>N</i> MePhe-Val- <i>N</i> MePhe] (4)	S7
Figure S9. ¹³ C NMR spectrum (100 MHz, CD ₃ OD) of cyclo[Val- <i>N</i> MePhe-Val- <i>N</i> MePhe] (4)	S8
Figure S10. IR spectrum of cyclo[Val- <i>N</i> MePhe-Val- <i>N</i> MePhe] (4)	S8
Figure S11. Analytical RP-HPLC profile of cyclo[Ile- <i>N</i> MePhe-Val- <i>N</i> MePhe] (5)	S9
Figure S12. HRMS profile of synthetic cyclo[Ile- <i>N</i> MePhe-Val- <i>N</i> MePhe] (5)	S9
Figure S13. ¹ H NMR spectrum (400 MHz, CD ₃ OD) of cyclo[Ile- <i>N</i> MePhe-Val- <i>N</i> MePhe] (5)	S10
Figure S14. ¹³ C NMR spectrum (100 MHz, CD ₃ OD) of cyclo[Ile- <i>N</i> MePhe-Val- <i>N</i> MePhe] (5)	S10
Figure S15. IR spectrum of cyclo[Ile- <i>N</i> MePhe-Val- <i>N</i> MePhe] (5)	S11
Figure S16. Analytical RP-HPLC profile of cyclo[Leu- <i>N</i> MePhe-Leu- <i>N</i> MePhe] (6)	S11
Figure.S17. HRMS profile of cyclo[Leu- <i>N</i> MePhe-Leu- <i>N</i> MePhe] (6)	S12
Figure S18. ¹ H NMR spectrum (400 MHz, CDCl ₃) of cyclo[Leu- <i>N</i> MePhe-Leu- <i>N</i> MePhe] (6)	S12
Figure S19. ¹³ C NMR spectrum (100 MHz, CDCl ₃) of cyclo[Leu- <i>N</i> MePhe-Leu- <i>N</i> MePhe] (6)	S13
Figure S20. COSY spectrum (400 MHz, CDCl ₃) of cyclo[Leu- <i>N</i> MePhe-Leu- <i>N</i> MePhe] (6)	S13
Figure S21. HSQC spectrum (400 MHz, CDCl ₃) of cyclo[Leu- <i>N</i> MePhe-Leu- <i>N</i> MePhe] (6)	S14
Figure S22. NOESY spectrum (400 MHz, CDCl ₃) of cyclo[Leu- <i>N</i> MePhe-Leu- <i>N</i> MePhe] (6)	S14
Figure S23. NOESY spectrum (400 MHz, d ₆ -DMSO) of cyclo[Leu- <i>N</i> MePhe-Leu- <i>N</i> MePhe] (6)	S15
Figure S24. IR spectrum of cyclo[Leu- <i>N</i> MePhe-Leu- <i>N</i> MePhe] (6)	S16
Figure S25. RP-HPLC-UV (210nm) profile of the T3P-mediated cyclisation of 9 at room temperature in CH ₂ Cl ₂	S16
Figure S26. RP-HPLC-UV (210 nm) profile of the T3P-mediated cyclisation of 9 at room temperature in EtOAc	S17
Figure S27. RP-HPLC-UV-ESIMS spectra of T3P-mediated cyclisation of 9 at 0 °C in DMF/CH ₂ Cl ₂	S18
Figure S28. RP-HPLC-UV (210 nm) traces of the reaction mixture obtained during the synthesis of 6 from its linear precursor 9 mediated by A) T3P, B) HBTU and C) HATU after 24 hr at room temperature.	S19
Figure S29. RP-HPLC-UV (210 nm) traces of the reaction mixture obtained during the synthesis of 6 from its linear precursor 9 mediated by HATU after 24 hr at 45 °C.	S19
Figure S30. RP-HPLC-UV (210 nm) profile of the reaction mixture of 9 , T3P (1 equiv.) and DIPEA (2 equiv.) in CD ₂ Cl ₂ after 30 min. at 5 °C	S20
Figure S31. HRMS profile of cyclo[Leu- <i>N</i> MePhe-Leu- <i>N</i> MePhe] (6a , 6b)	S21
Figure S32. HRMS/MS profile of cyclo[Leu- <i>N</i> MePhe-Leu- <i>N</i> MePhe] (6a , 6b)	S21
Figure S33. ¹ H NMR spectra (500 MHz, CD ₂ Cl ₂) of the cyclisation of 9 (2 mM) with T3P (1 equiv.) and DIPEA (3 equiv.) at 5, 27 and 45 °C.	S22
Figure S34. ¹ H and 1D NOE NMR spectra (500 MHz, CD ₂ Cl ₂ , 27 °C) of the reaction mixture	S23

of 9 (2 mM), T3P (1 equiv.) and DIPEA (2 equiv.) in CD ₂ Cl ₂ after 30 min at 5 °C.	
Figure S35. ¹ H NMR spectra (500 MHz, CD ₂ Cl ₂ , 45 °C) of the reaction mixture of 9 (2 mM), T3P (1 equiv.) and DIPEA (2 equiv.) in CD ₂ Cl ₂ at different time points. The spectrum shows the C ^α H proton region.	S24
Figure S36. Analytical RP-HPLC profile of cyclo[Leu- <i>N</i> MePhe-Val- <i>N</i> MePhe] (7)	S25
Figure S37. HRMS profile of synthetic cyclo[Leu- <i>N</i> MePhe-Val- <i>N</i> MePhe] (7)	S25
Figure.S38. ¹ H NMR spectrum (400 MHz, CDCl ₃) of cyclo[Leu- <i>N</i> MePhe-Val- <i>N</i> MePhe] (7)	S26
Figure.S39. ¹³ C NMR spectrum (100 MHz, CDCl ₃) of cyclo[Leu- <i>N</i> MePhe-Val- <i>N</i> MePhe] (7)	S26
Figure S40. COSY spectrum (400 MHz, CDCl ₃) of cyclo[Leu- <i>N</i> MePhe-Val- <i>N</i> MePhe] (7)	S27
Figure S41. NOESY spectrum (400 MHz, CDCl ₃) of cyclo[Leu- <i>N</i> MePhe-Val- <i>N</i> MePhe] (7)	S27
Figure S42. IR spectrum of cyclo[Leu- <i>N</i> MePhe-Val- <i>N</i> MePhe] (7)	S28
Figure S43. ¹ H NMR spectrum (500 MHz, CD ₃ OD) of cyclo[D-Leu- <i>N</i> MePhe-Leu- <i>N</i> MePhe] (6 [*])	S28
Figure S44. The dose-dependent inhibition of five cyclotetrapeptides against mouse myeloma cells	S29
Table S1. Optimized structures of the different conformers of 6 [*] in a tube representation (top). Potential energy differences relative to the <i>tctc</i> conformer (in kcal/mol) and dipole moments (given in parenthesis in Debye) of the three minimised conformers of 6 in <i>vacuum</i> , DMSO and CH ₂ Cl ₂ .	S29
Table S2. Potential energy (in kcal/mol) and dipole moments of the three minimised conformers of 6 in <i>vacuum</i> , DMF and CH ₂ Cl ₂	S29

Cyclo[Ile-NMePhe-Ile-NMePhe] (3)

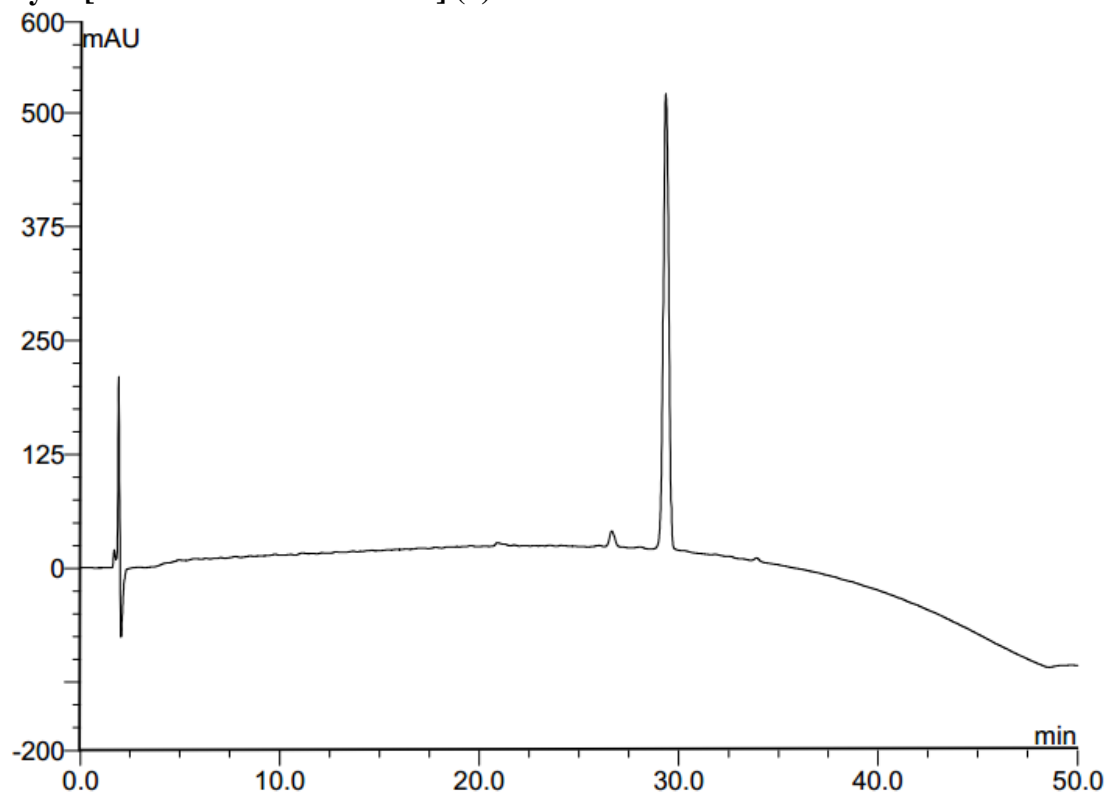


Figure S1. Analytical RP-HPLC profile of cyclo[Ile-NMePhe-Ile-NMePhe] (**3**); linear gradient of 5%B-95%B over 45 min (*ca.* 2 %B•min⁻¹), 1 mL•min⁻¹, using XTerra MS C₁₈ column (4.6 mm × 150 mm, 5 μm).

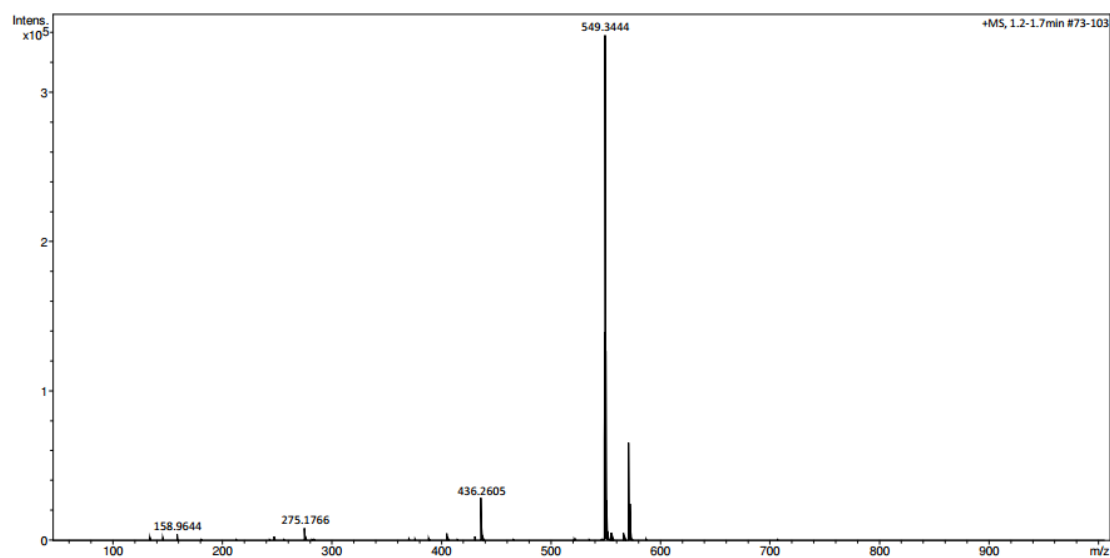


Figure.S2. HRMS profile of synthetic cyclo[Ile-NMePhe-Ile-NMePhe] (**3**)

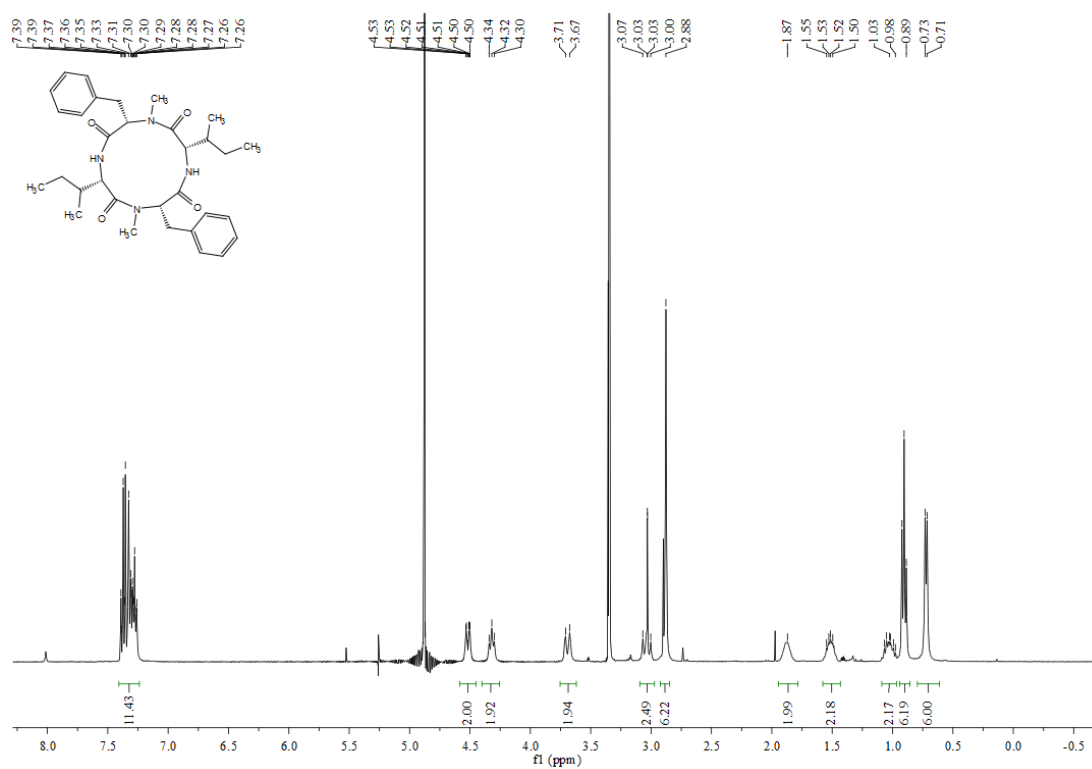


Figure.S3. ¹H NMR spectrum (400 MHz, CD₃OD) of cyclo[Ile-NMePhe-Ile-NMePhe] (3)

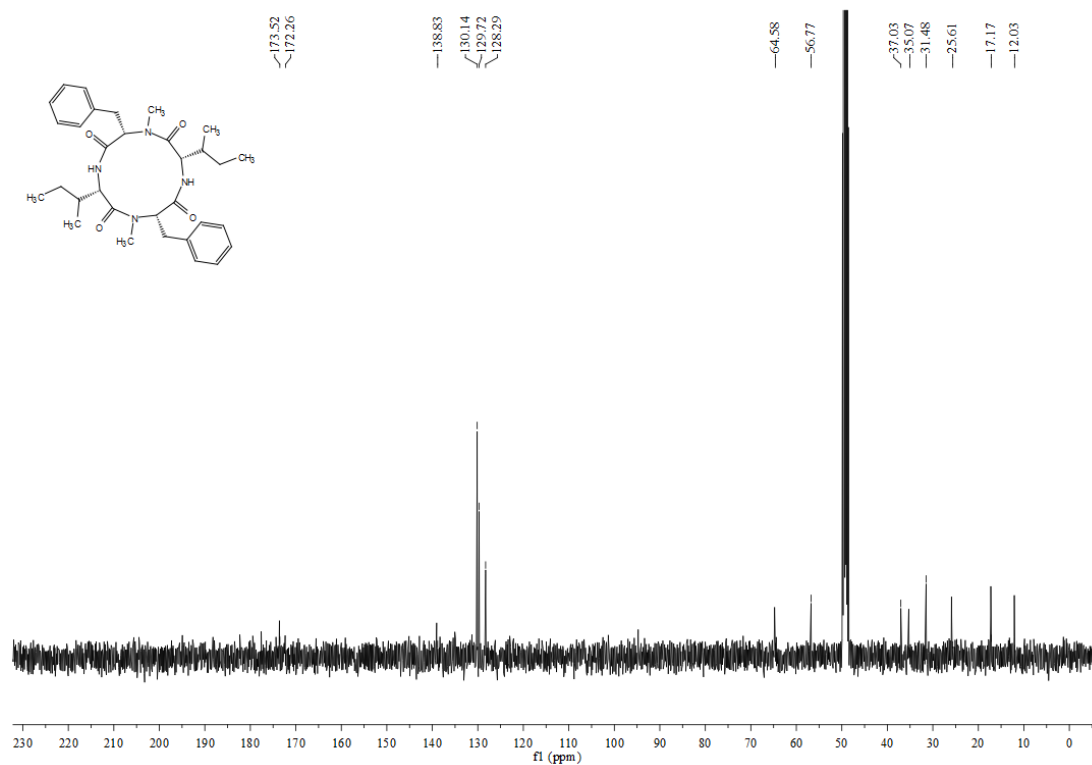


Figure.S4. ¹³C NMR spectrum (100 MHz, CD₃OD) of cyclo[Ile-NMePhe-Ile-NMePhe] (3)

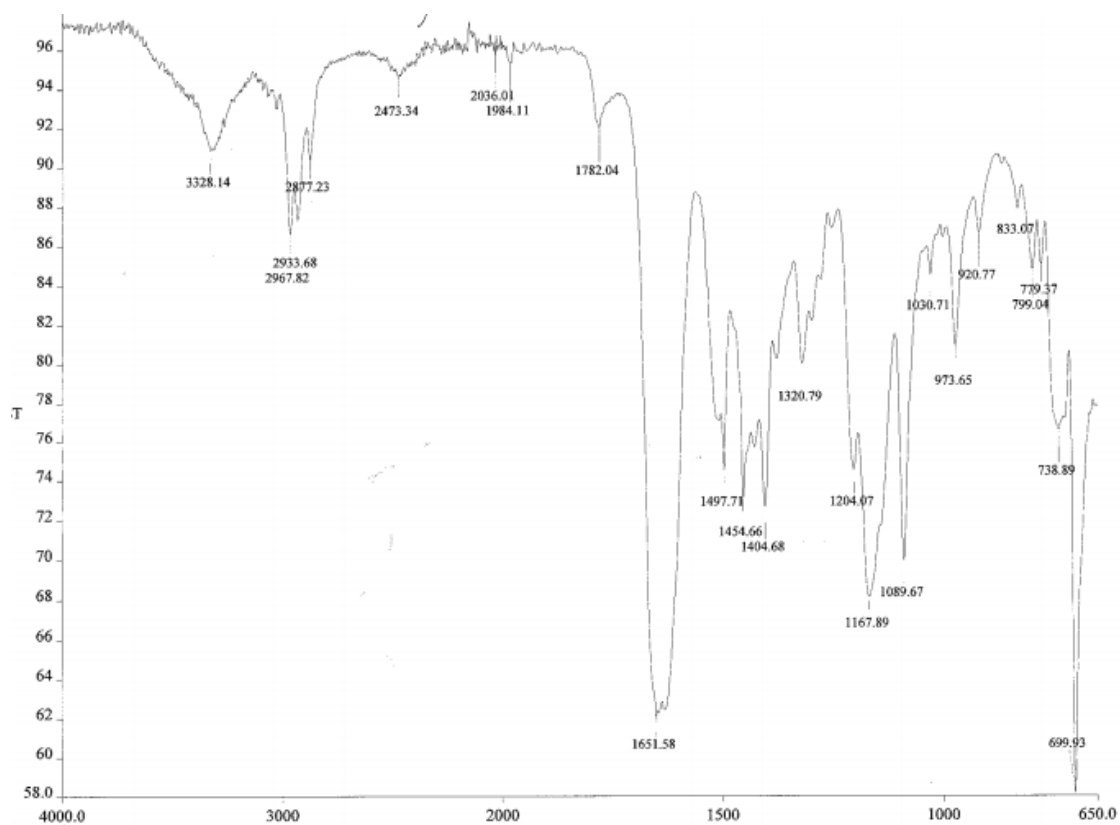


Figure.S5. IR spectrum of cyclo[Ile-NMePhe-Ile-NMePhe] (3)

Cyclo[Val-NMePhe-Val-NMePhe] (4)

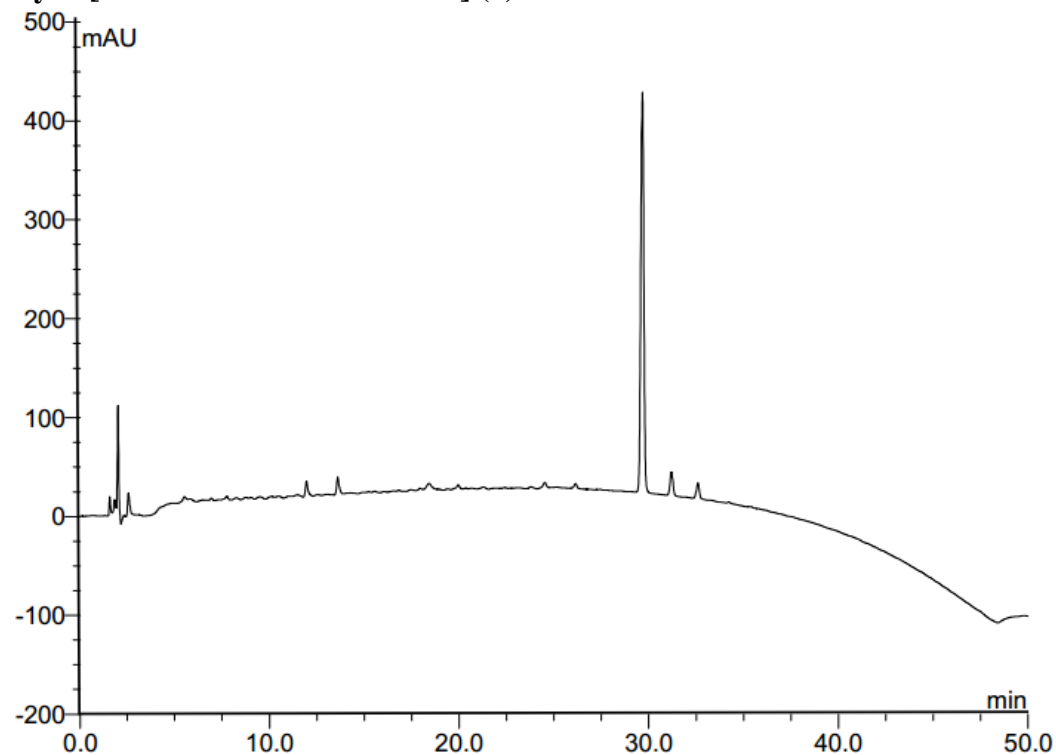


Figure S6. Analytical RP-HPLC profile of cyclo[Val-NMePhe-Val-NMePhe] (4); linear gradient of 5%B-95%B over 45 min (*ca.* 2 %B•min⁻¹), 1 mL•min⁻¹, using XTerra MS C₁₈ column (4.6 mm × 150 mm, 5 μm).

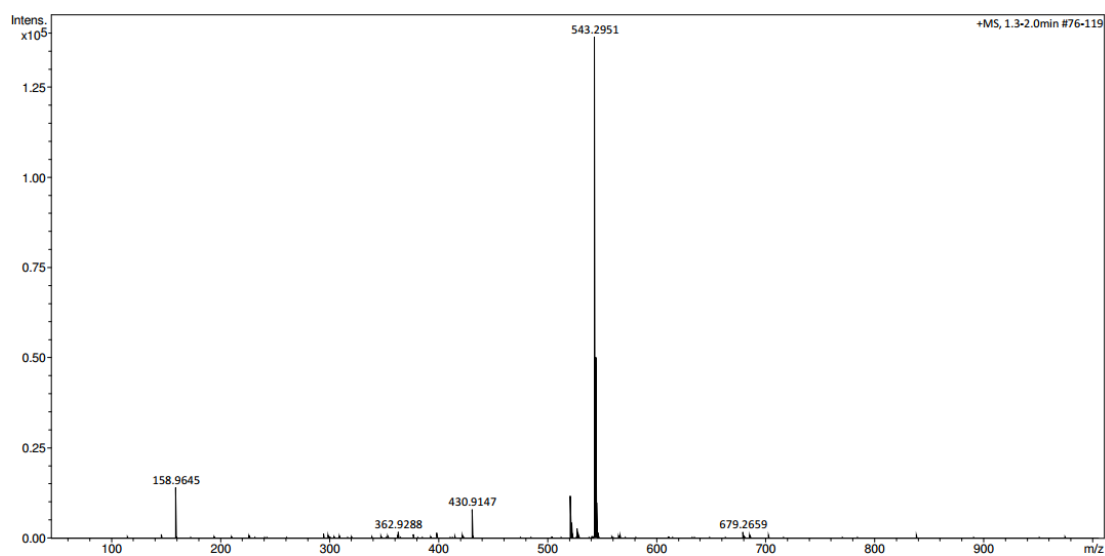


Figure.S7. HRMS profile of cyclo[Val-NMePhe-Val-NMePhe] (**4**)

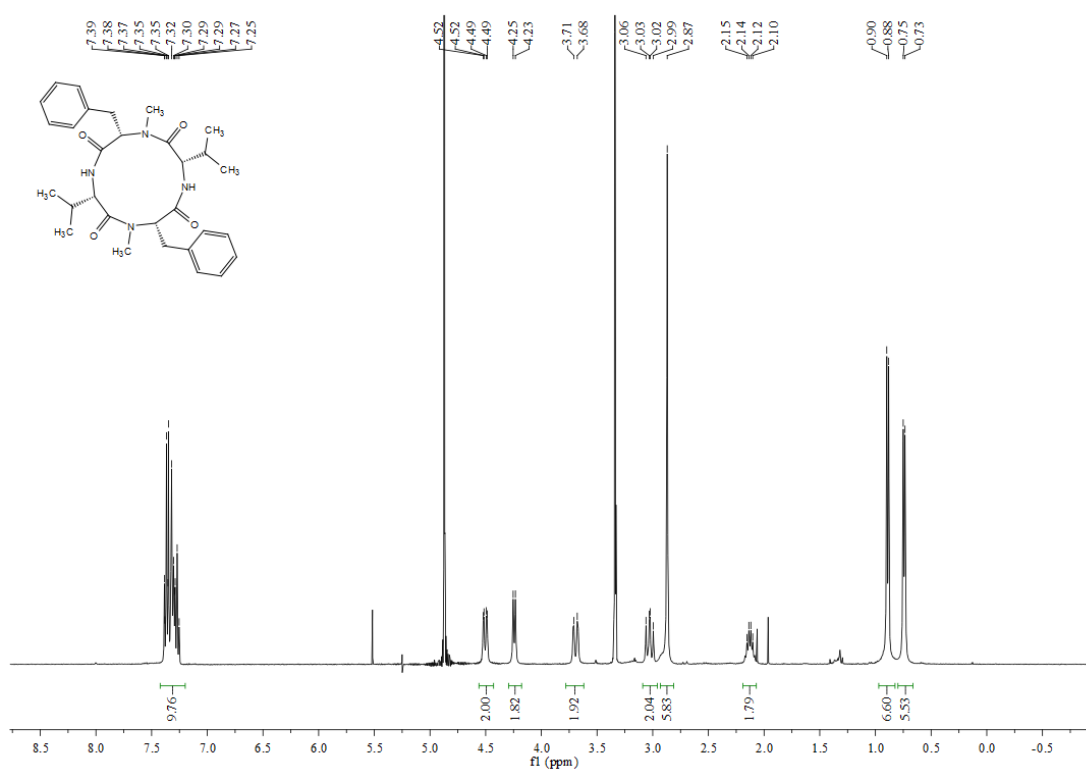


Figure.S8. ^1H NMR spectrum (400 MHz, CD_3OD) of cyclo[Val-NMePhe-Val-NMePhe] (**4**)

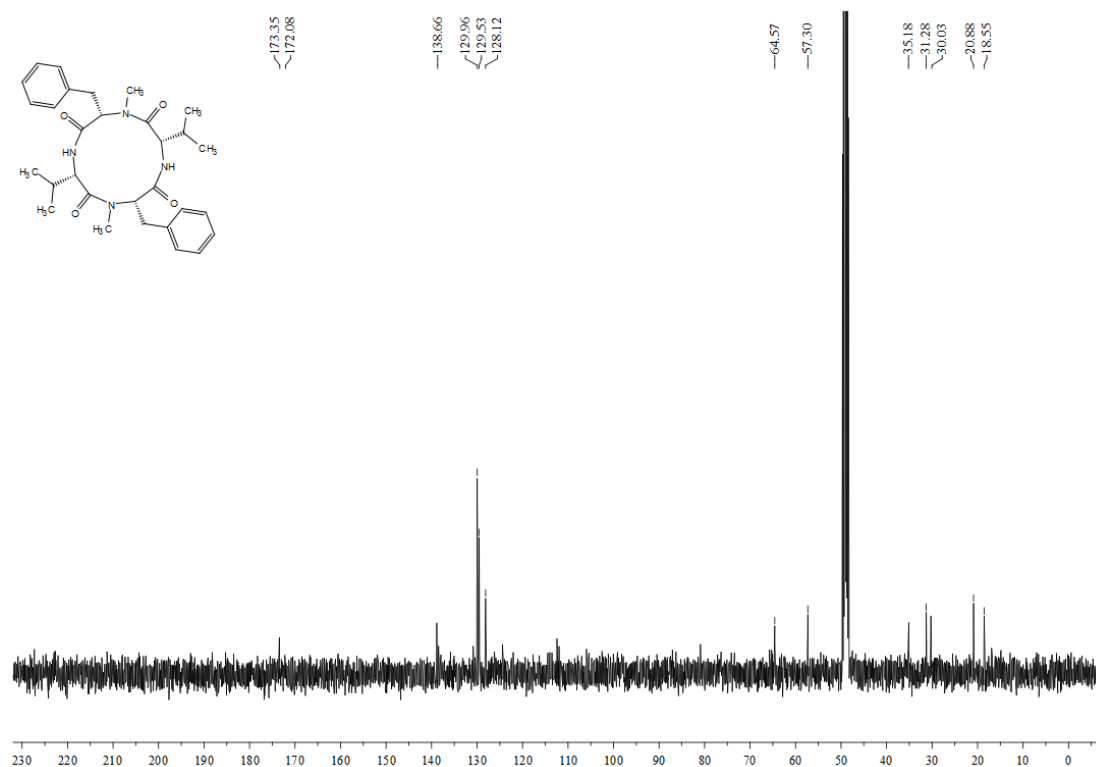


Figure.S9. ¹³C NMR spectrum (100 MHz, CD₃OD) of cyclo[Val-NMePhe-Val-NMePhe] (4)

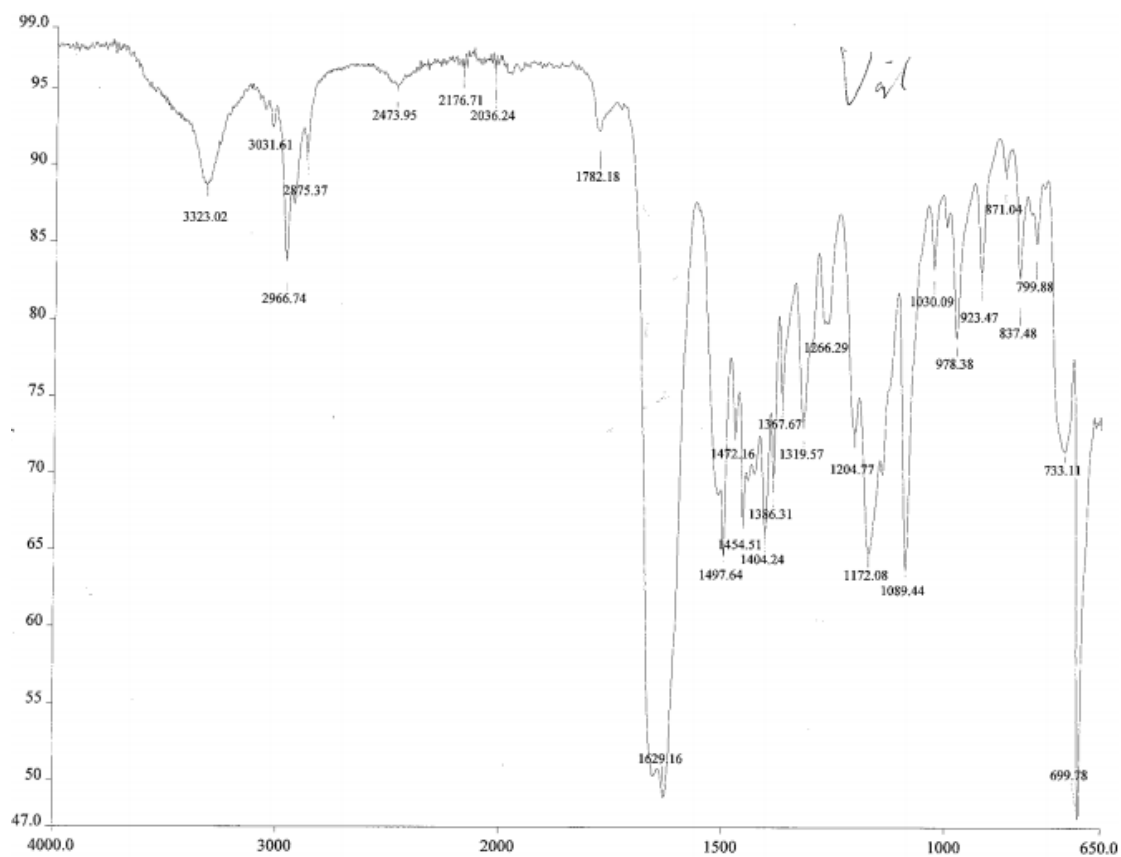


Figure.S10. IR spectrum of cyclo[Val-NMePhe-Val-NMePhe] (4)

Cyclo[Ile-NMePhe-Val-NMePhe] (5)

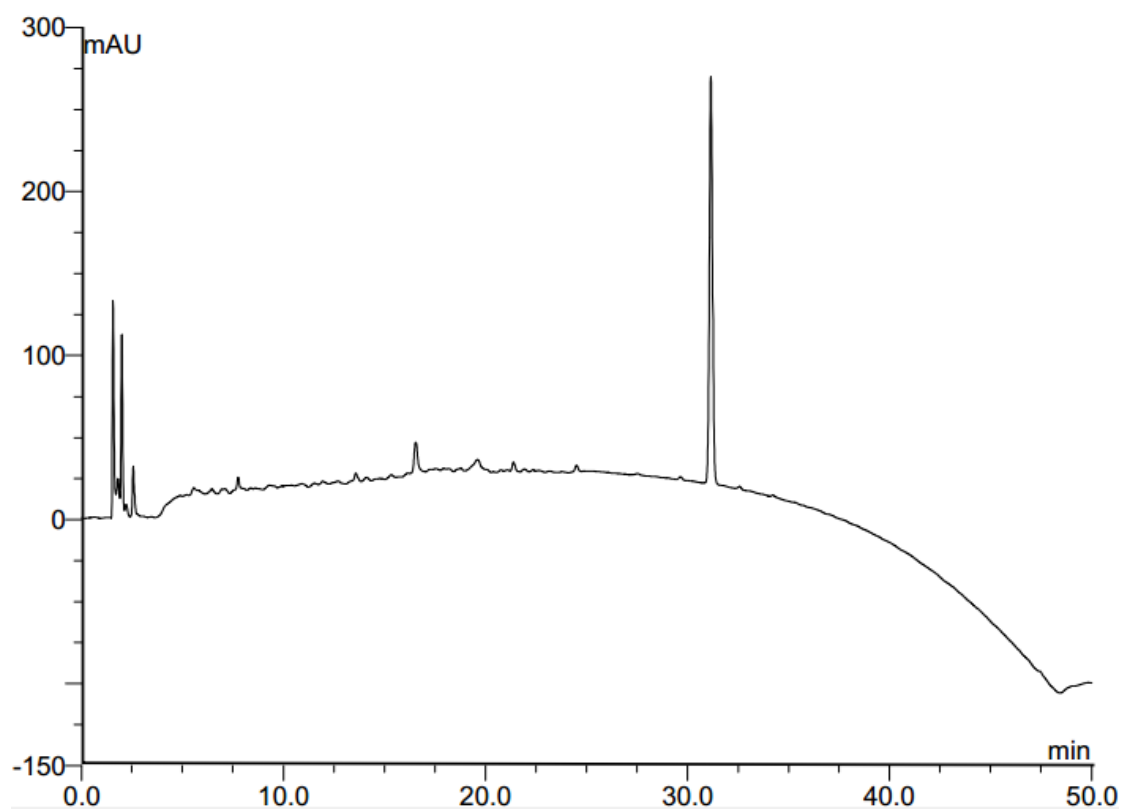


Figure S11. Analytical RP-HPLC profile of cyclo[Ile-NMePhe-Val-NMePhe] (**5**); linear gradient of 5%B-95%B over 45 min (*ca.* 2 %B•min⁻¹), 1 mL•min⁻¹, using XTerra MS C₁₈ column (4.6 mm × 150 mm, 5 μm).

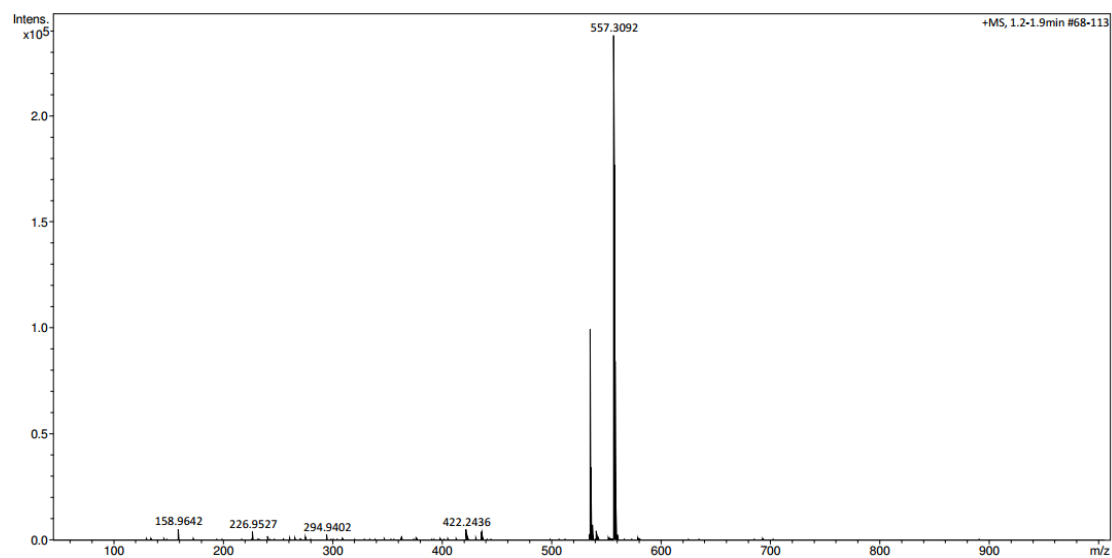


Figure.S12. HRMS profile of cyclo[Ile-NMePhe-Val-NMePhe] (**5**)

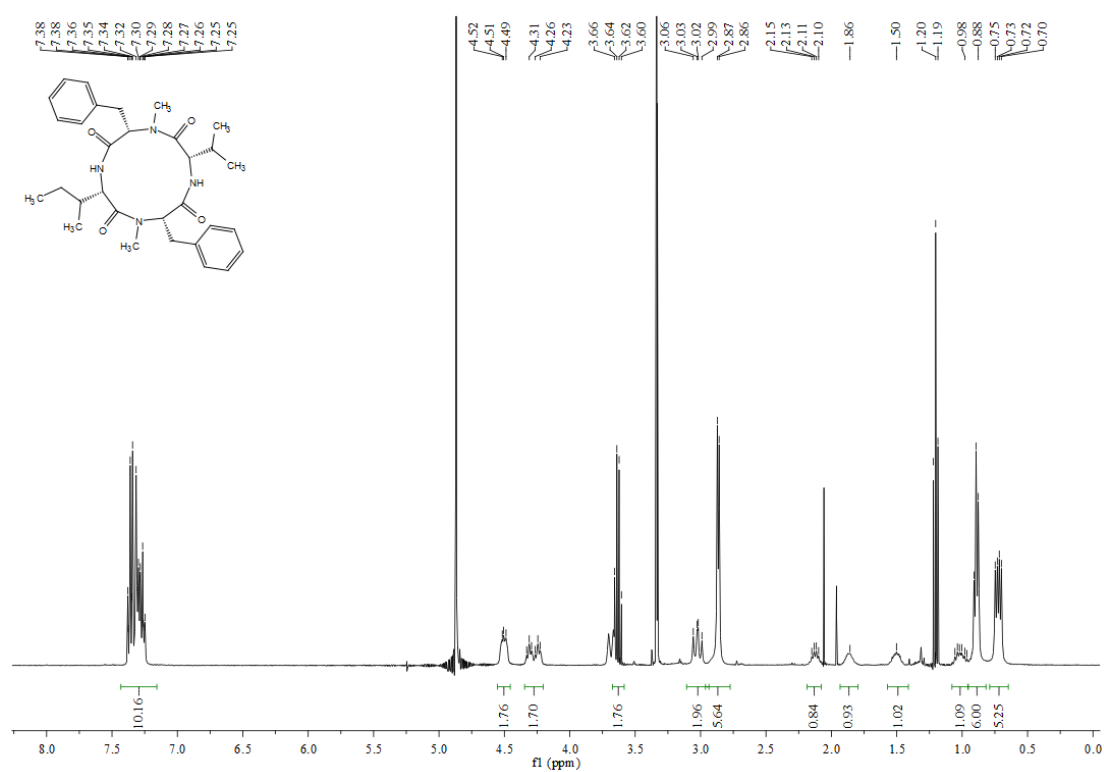


Figure.S13. ^1H NMR spectrum (400 MHz, CD_3OD) of cyclo[Ile-NMePhe-Val-NMePhe] (5)

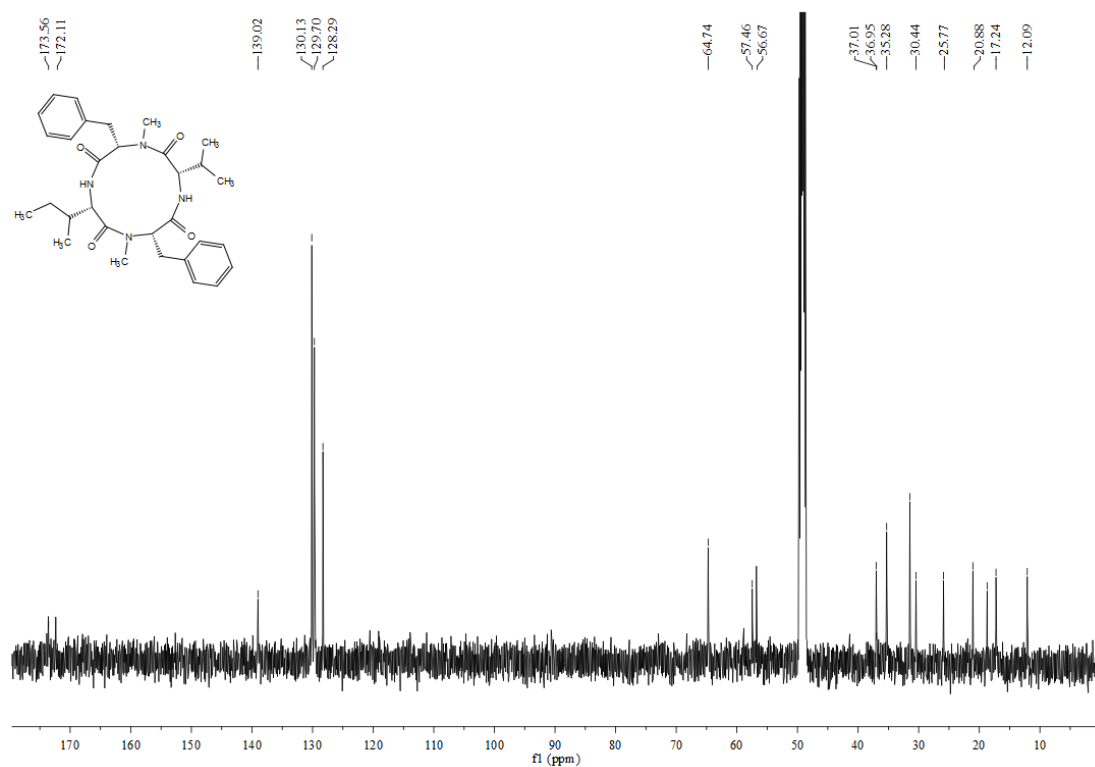


Figure.S14. ^{13}C NMR spectrum (125 MHz, CD_3OD) of cyclo[Ile-NMePhe-Val-NMePhe] (5)

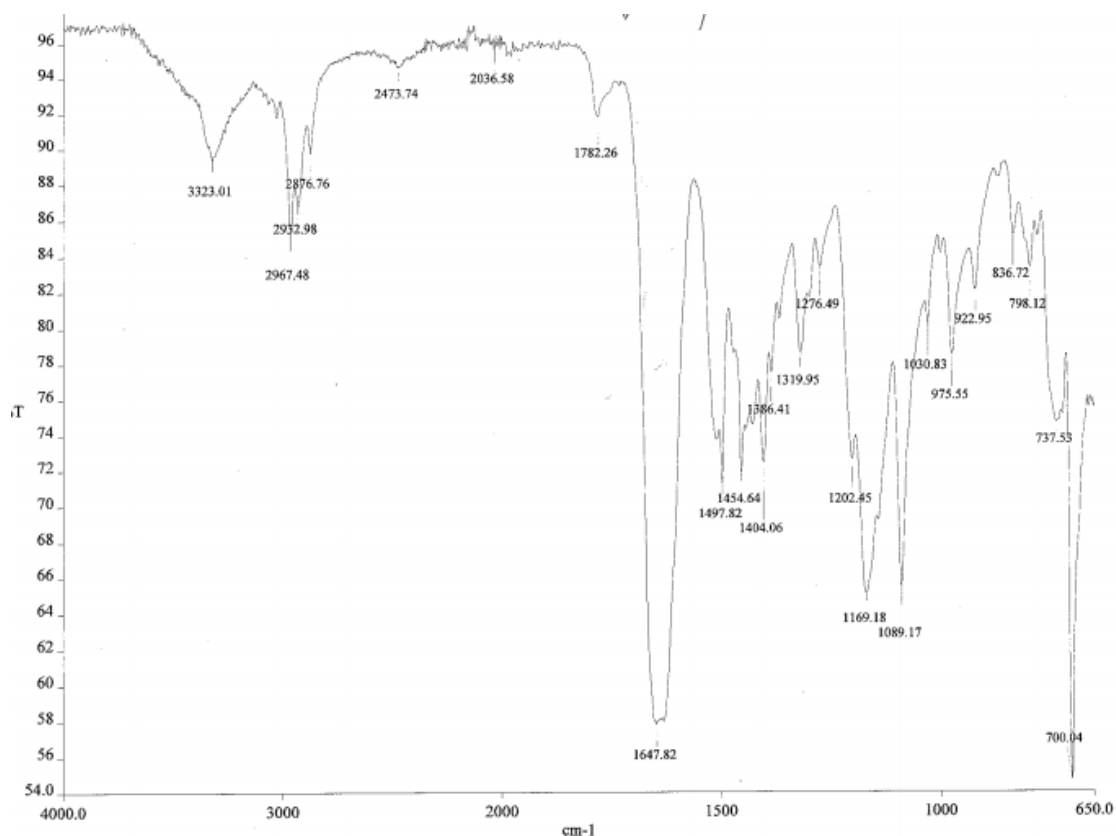


Figure.S15. IR spectrum of cyclo[Ile-NMePhe-Val-NMePhe] (5)

Cyclo[Leu-NMePhe-Leu-NMePhe] (6)

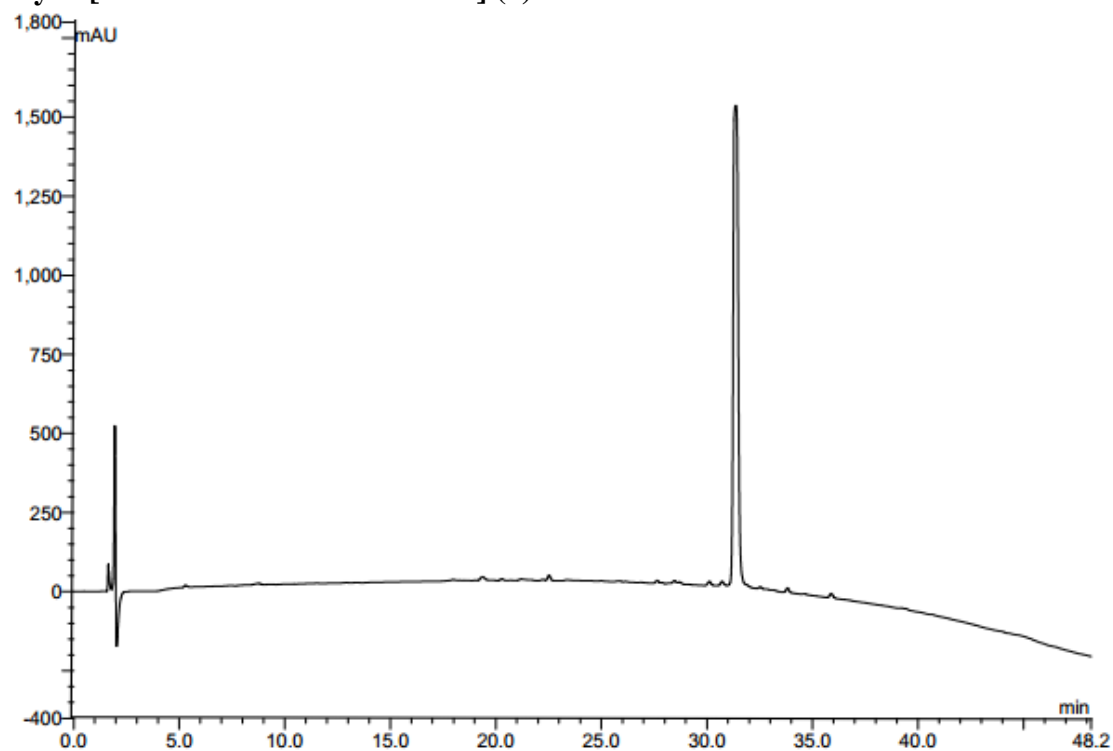


Figure S16. Analytical RP-HPLC profile of cyclo[Leu-NMePhe-Leu-NMePhe] (6); linear gradient of 5%B-95%B over 45 min (*ca.* 2 %B•min⁻¹), 1 mL•min⁻¹, using XTerra MS C₁₈ column (4.6 mm

× 150 mm, 5 μm).

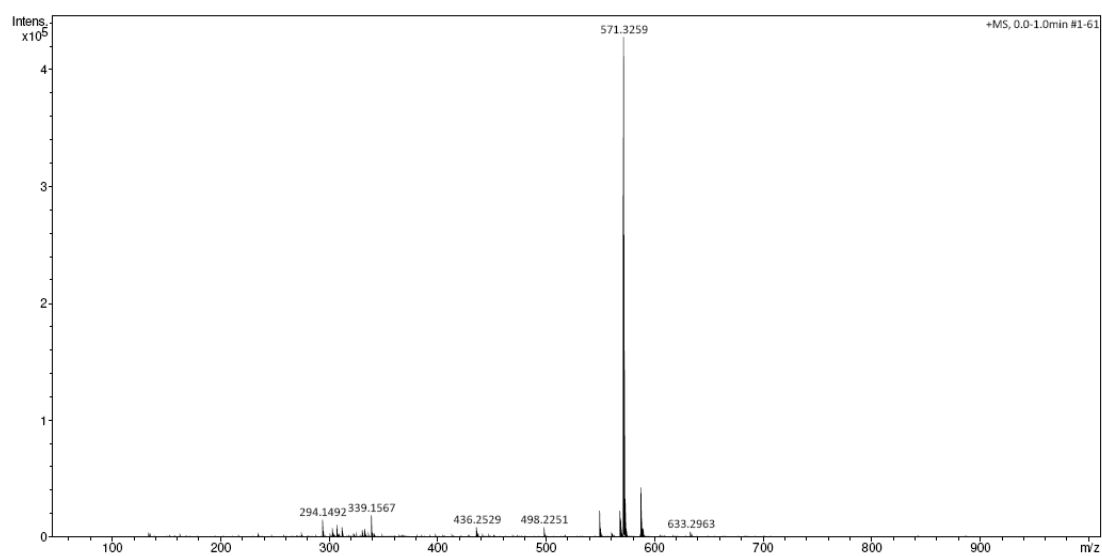


Figure S17. HRMS profile of cyclo[Leu-NMePhe-Leu-NMePhe] (6)

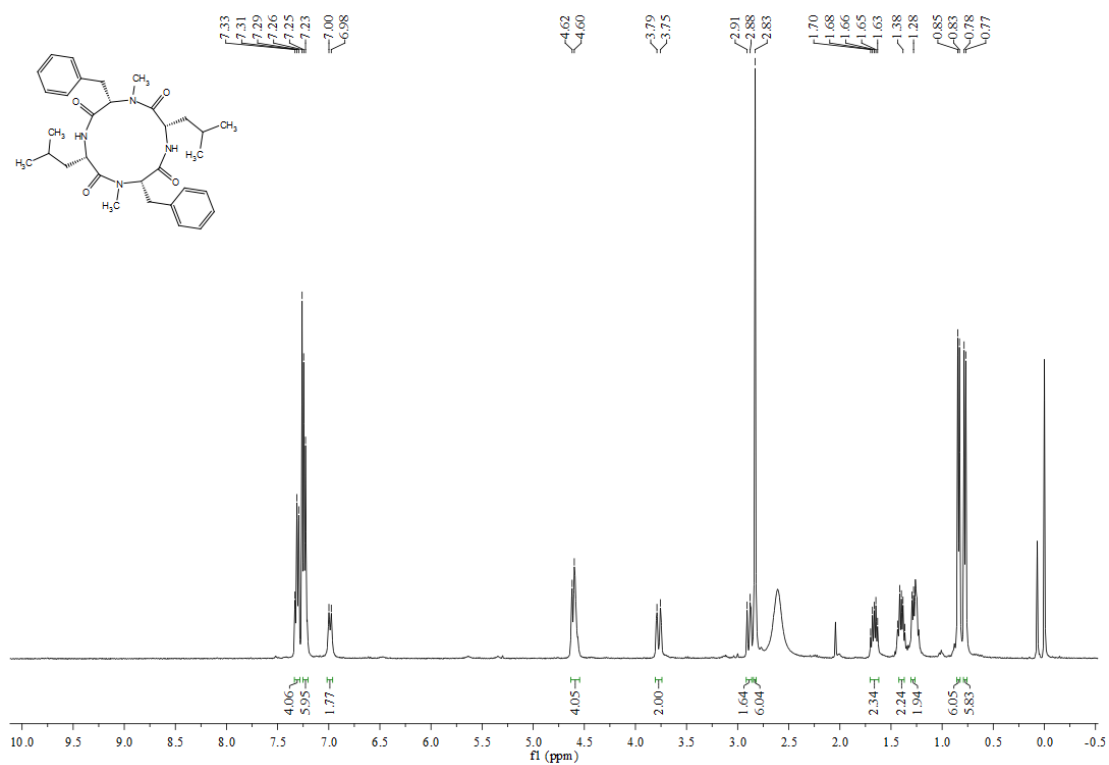


Figure.S18. ¹H NMR spectrum (400 MHz, CDCl₃) of cyclo[Leu-NMePhe-Leu-NMePhe] (6)

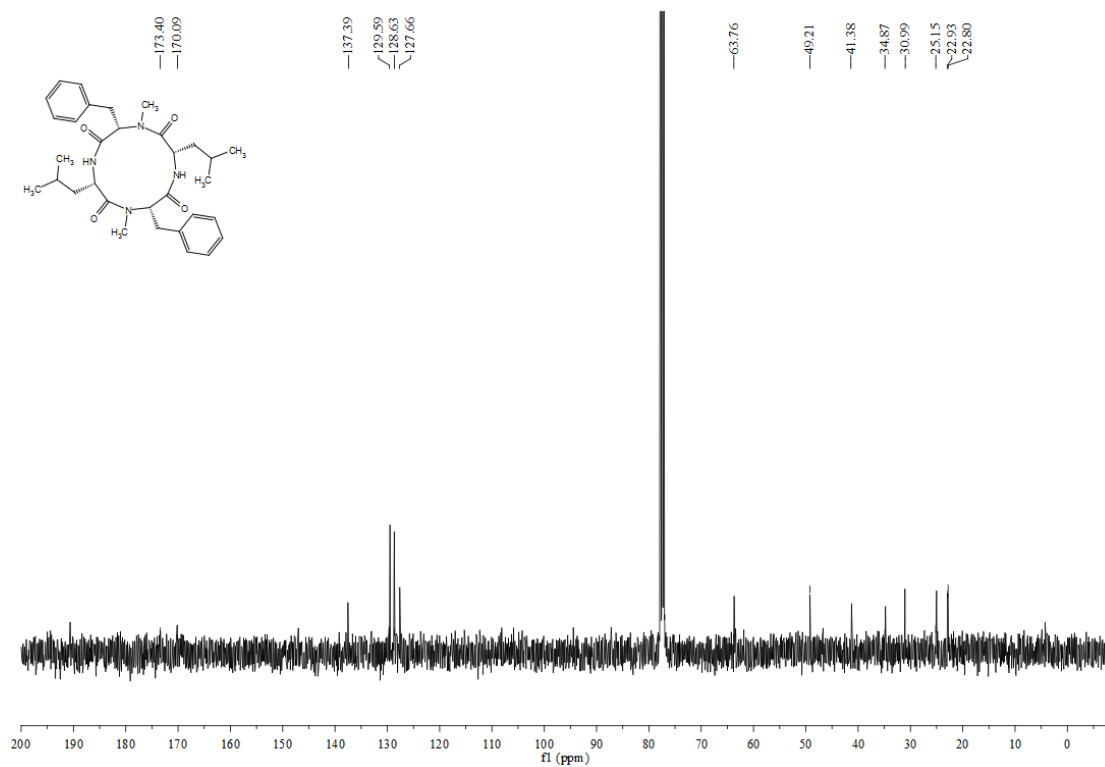


Figure S19. ^{13}C NMR spectrum (100 MHz, CDCl_3) of cyclo[Leu-NMePhe-Leu-NMePhe] (6)

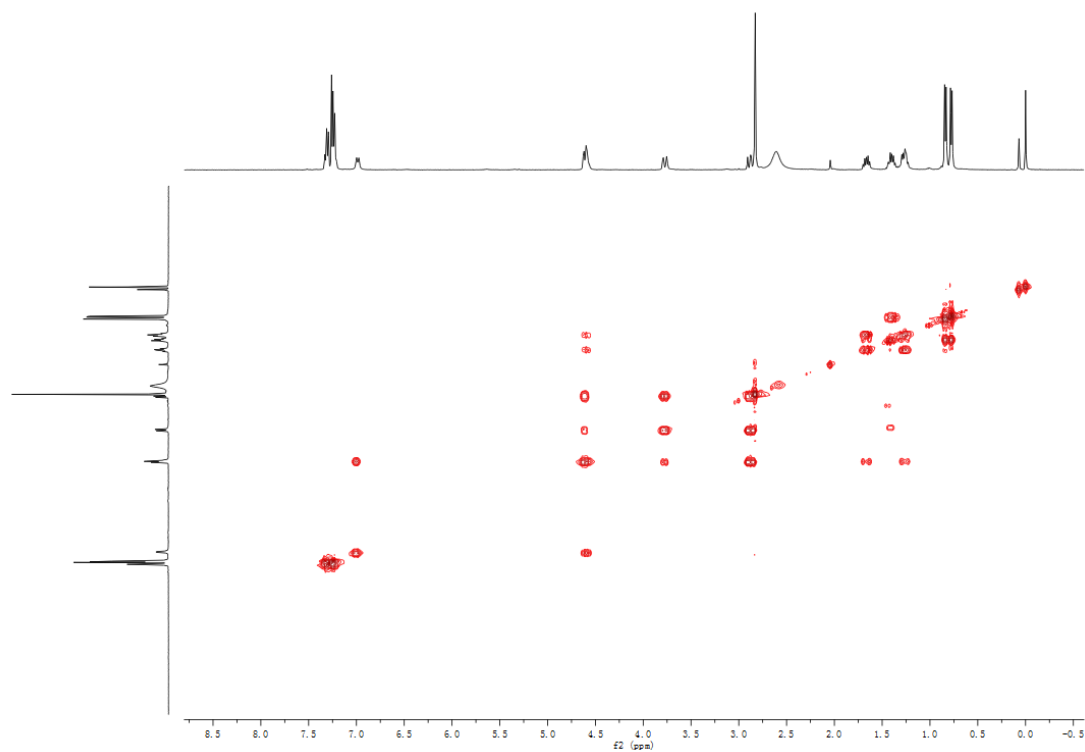


Figure S20. COSY spectrum (400 MHz, CDCl_3) of cyclo[Leu-NMePhe-Leu-NMePhe] (6)

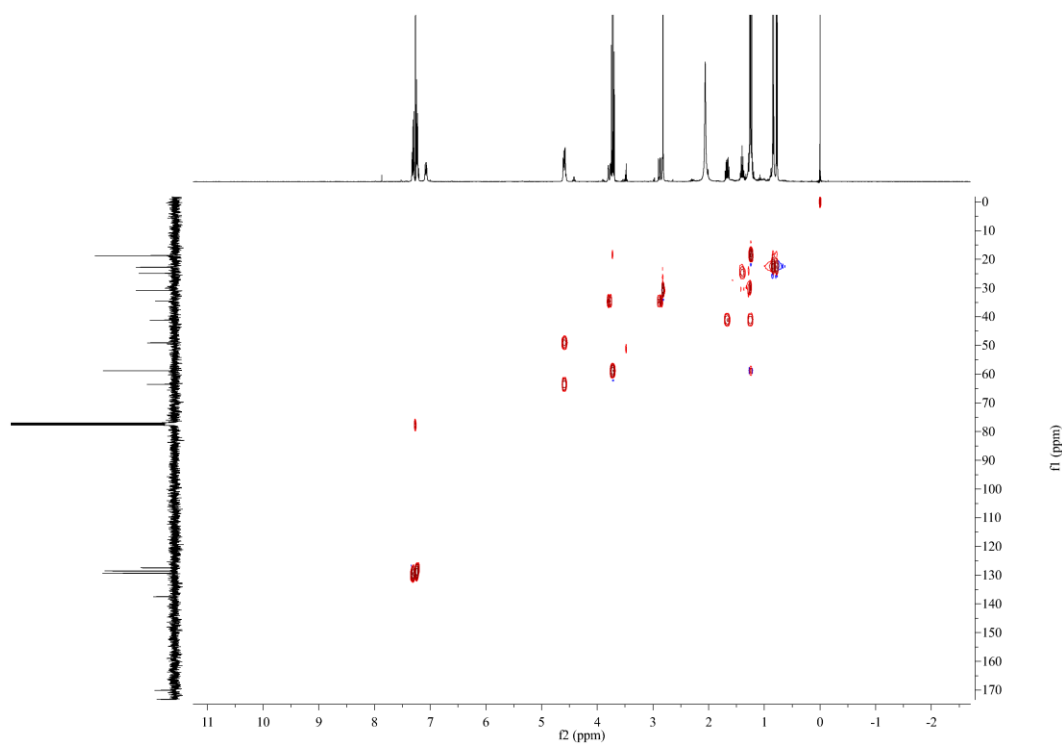


Figure S21. HSQC spectrum (400 MHz, CDCl_3) of cyclo[Leu-*N*MePhe-Leu-*N*MePhe] (**6**)

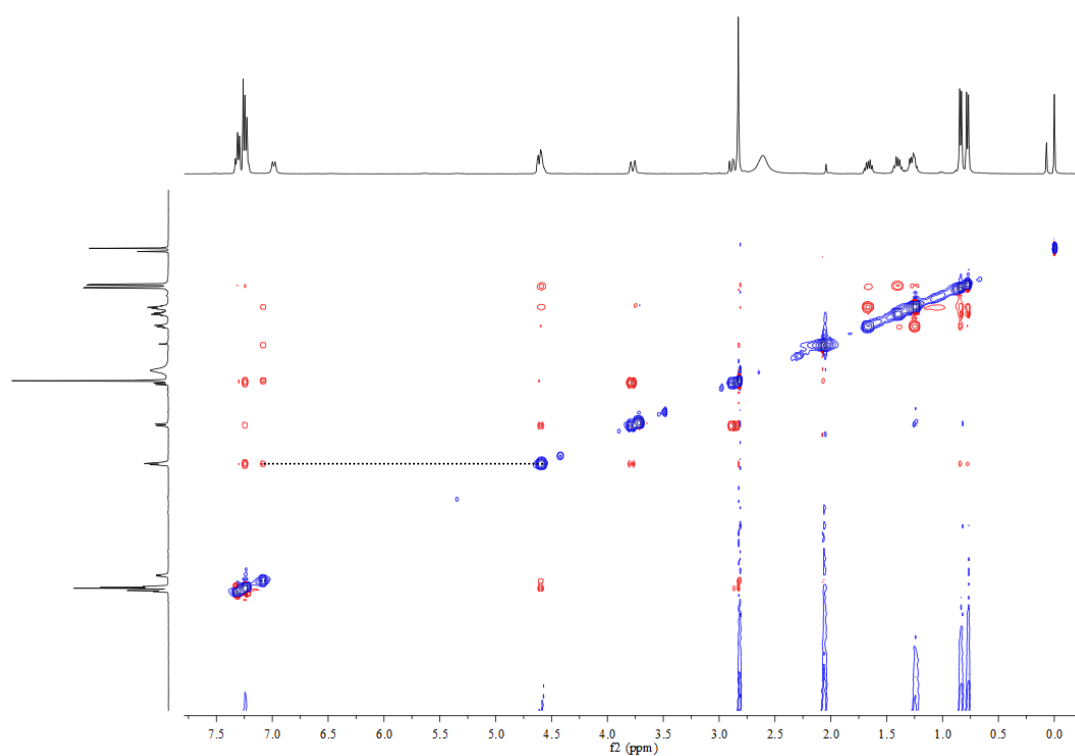


Figure S22. NOESY (400 MHz, CDCl_3) spectrum of cyclo[Leu-*N*MePhe-Leu-*N*MePhe] (**6**)

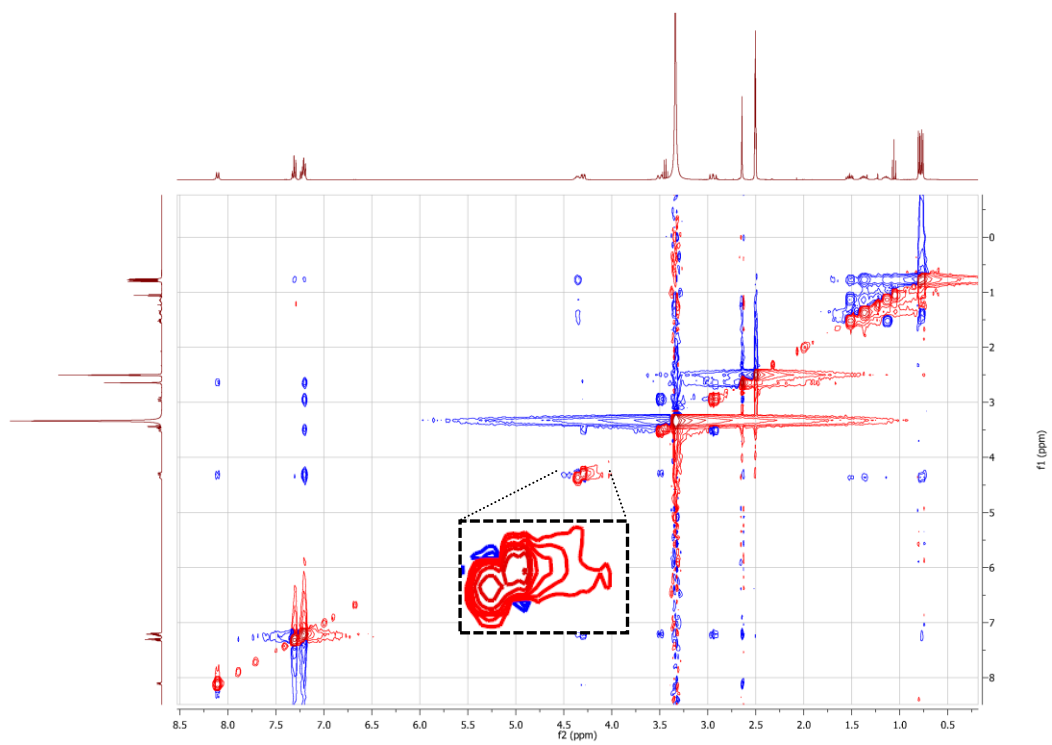


Figure S23. NOESY (400 MHz, d_6 -DMSO) spectrum of cyclo[Leu-NMePhe-Leu-NMePhe] (**6**)

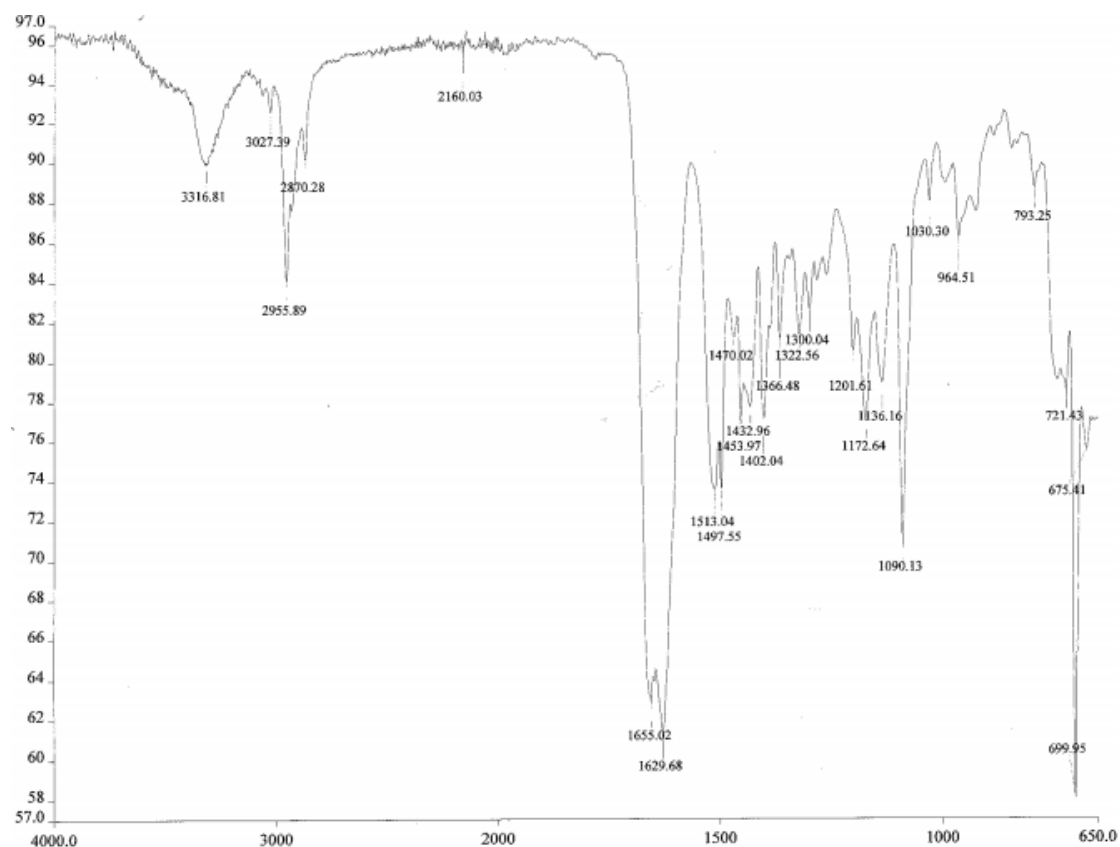


Figure S24. IR spectrum of cyclo[Leu-NMePhe-Leu-NMePhe] (**6**)

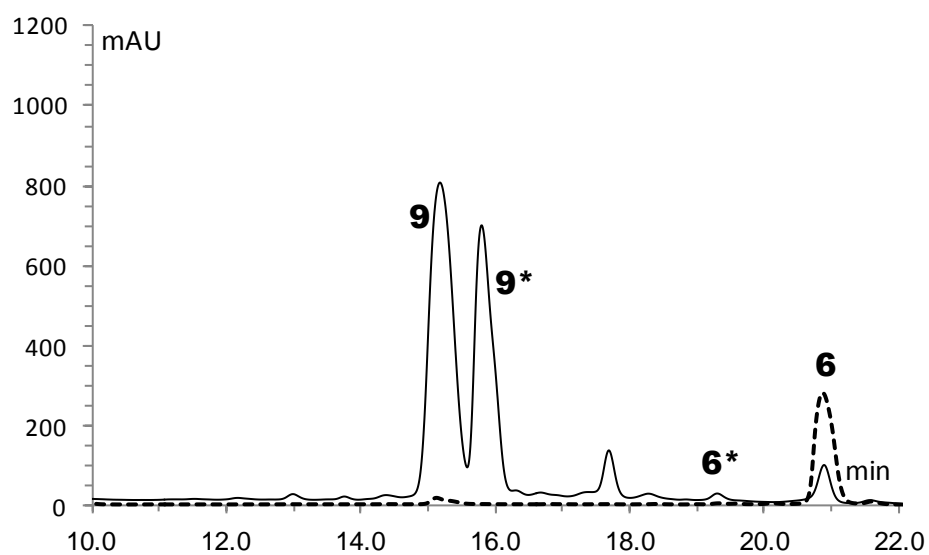


Figure S25. RP-HPLC-UV (210nm) profile of the T3P-mediated cyclisation of **9** at room temperature in CH₂Cl₂; linear gradient of 5%B-95%B over 30 min (ca. 3 %B•min⁻¹), 1 mL•min⁻¹, using XTerra MS C18 column (4.6 mm × 150 mm, 5 μm). A = 0.1% TFA in H₂O and B = 0.1 % TFA in ACN. Reaction conditions: 5 equiv. T3P, 6 equiv. DIPEA, CH₂Cl₂, 24 hours. The dashed line corresponds to the profile of a standard of **6**.

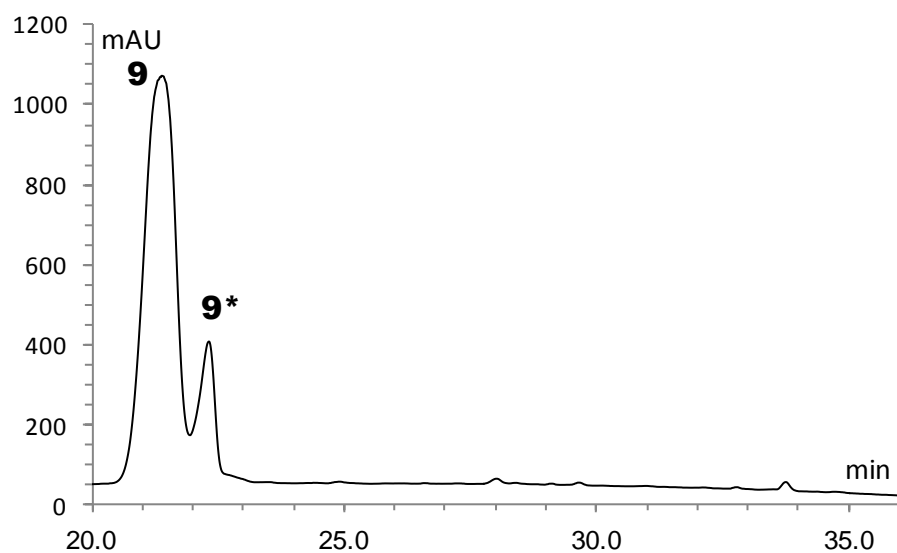


Figure S26. RP-HPLC-UV (210 nm) profile of the T3P-mediated cyclisation of **9** at room temperature in EtOAc; linear gradient of 5%B-95%B over 45 min (ca. 2 %B•min⁻¹), 1 mL•min⁻¹, using XTerra MS C18 column (4.6 mm × 150 mm, 5 μm). A = 0.1% TFA in H₂O and B = 0.1 % TFA in ACN. Reaction conditions: 5 equiv. T3P, 6 equiv. DIPEA, EtOAc, 1 day.

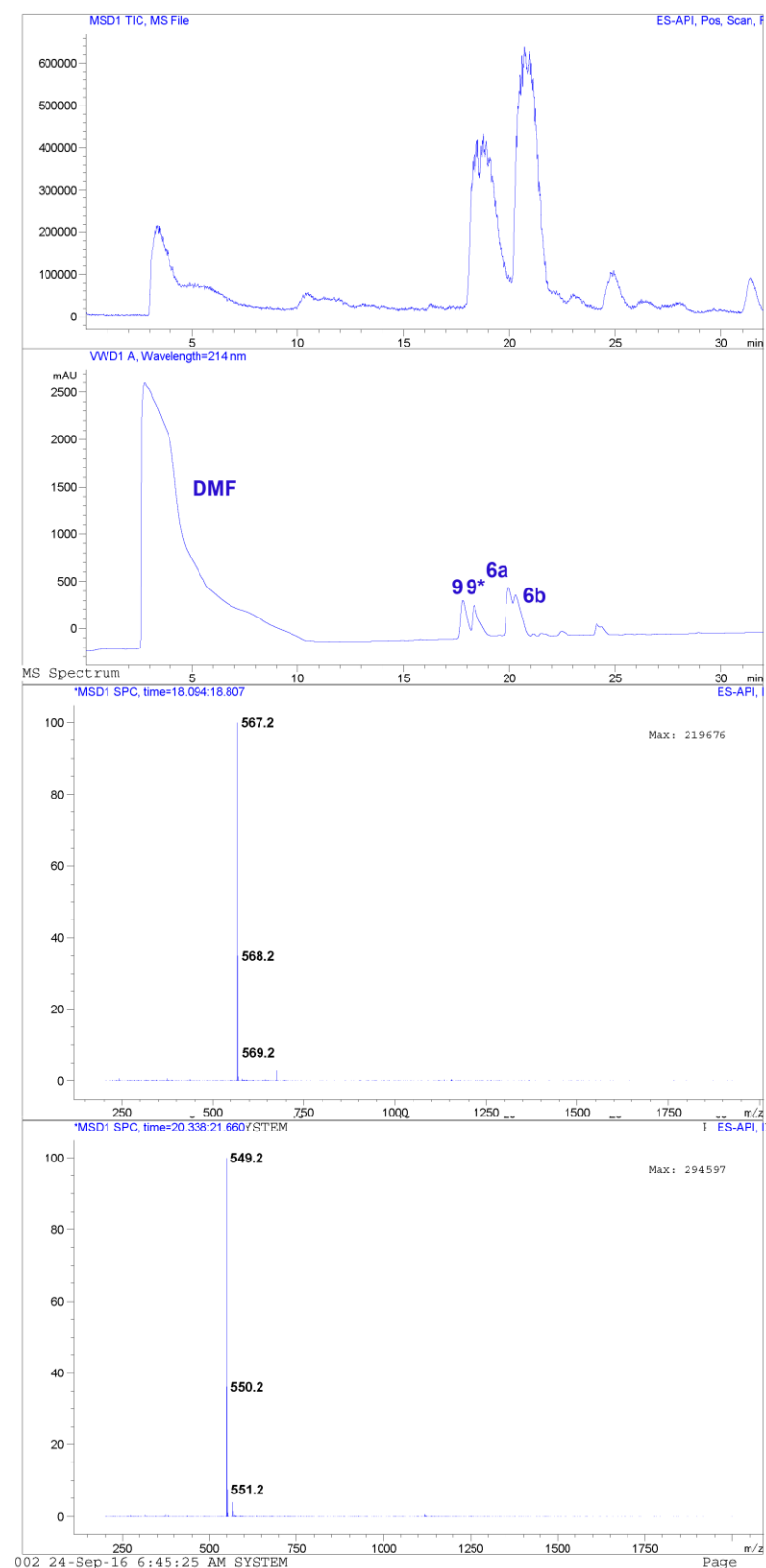


Figure S27. RP-HPLC-UV-ESIMS spectra of T3P-mediated cyclisation of **9** at 0 °C in DMF/CH₂Cl₂; linear gradient of 5%B-95%B over 30 min (3 %B•min⁻¹), 1 mL•min⁻¹, using a ZORBAX C3 column (3.0 mm × 150 mm, 3.5 μm). A = 0.1% formic acid in H₂O and B = 0.1 % formic acid in ACN. Reaction conditions: 5 equiv. T3P, 6 equiv. DIPEA, DMF/CH₂Cl₂, 1 day.

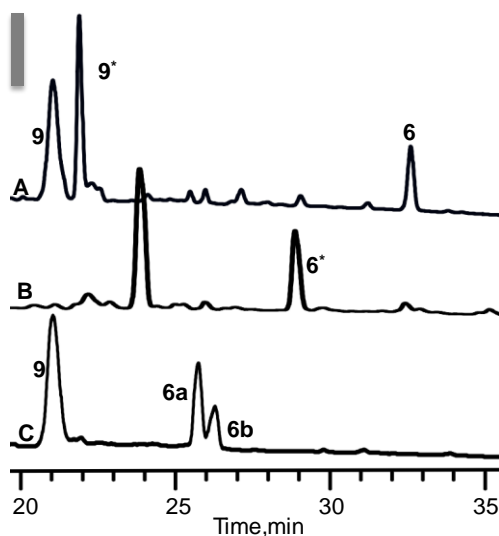


Figure S28. RP-HPLC-UV (210 nm) traces of the reaction mixture obtained during the synthesis of **6** from its linear precursor **9** mediated by A) T3P, B) HBTU and C) HATU at room temperature; linear gradient of 5%B-95%B over 45 min (*ca.* 2 %B·min⁻¹), 1 mL·min⁻¹, using XTerra MS C₁₈ column (4.6 mm × 150 mm, 5 μm). A = 0.1% TFA in H₂O and B = 0.1 % TFA in ACN. Reaction conditions: 5 equiv. coupling reagent, 6 equiv. DIPEA, DMF/ CH₂Cl₂ (1:1), 1 day. The scale bar shown is equivalent to 300 mUA.

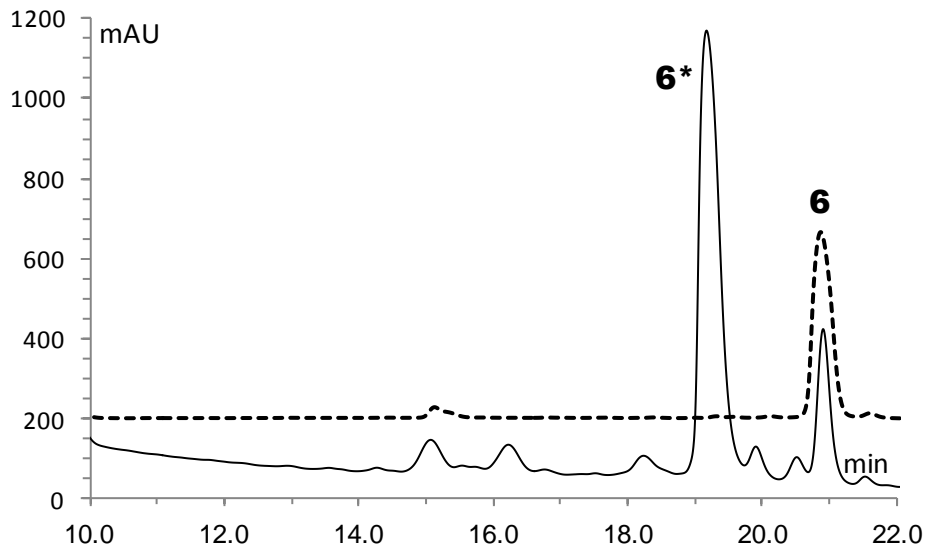


Figure S29. RP-HPLC-UV (210 nm) traces of the reaction mixture obtained during the synthesis of **6** from its linear precursor **9** mediated by HATU for 24 hr at 45 °C; linear gradient of 5%B-95%B over 30 min (*ca.* 3 %B·min⁻¹), 1 mL·min⁻¹, using XTerra MS C₁₈ column (4.6 mm × 150 mm, 5 μm). A = 0.1% TFA in H₂O and B = 0.1 % TFA in ACN. Reaction conditions: 5 equiv. coupling reagent, 6 equiv. DIPEA, DMF/ CH₂Cl₂ (1:1), 24 hr. The dashed line corresponds to the profile of a standard of **6**.

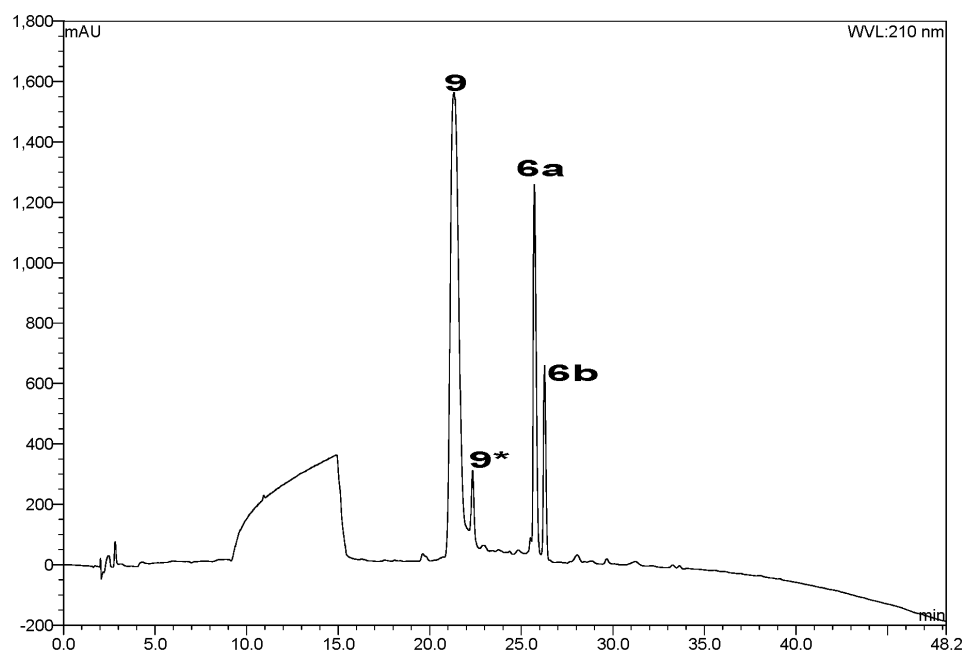


Figure S30 RP-HPLC-UV (210 nm) profile of the reaction mixture of **9**, T3P (1 equiv.) and DIPEA (2 equiv.) in CD_2Cl_2 after 30 min. at 5 °C; linear gradient of 5%B-95%B over 45 min (*ca.* 2 %B·min⁻¹), 1 mL·min⁻¹, using XTerra MS C₁₈ column (4.6 mm × 150 mm, 5 μm). A = 0.1% TFA in H₂O and B = 0.1 % TFA in ACN.

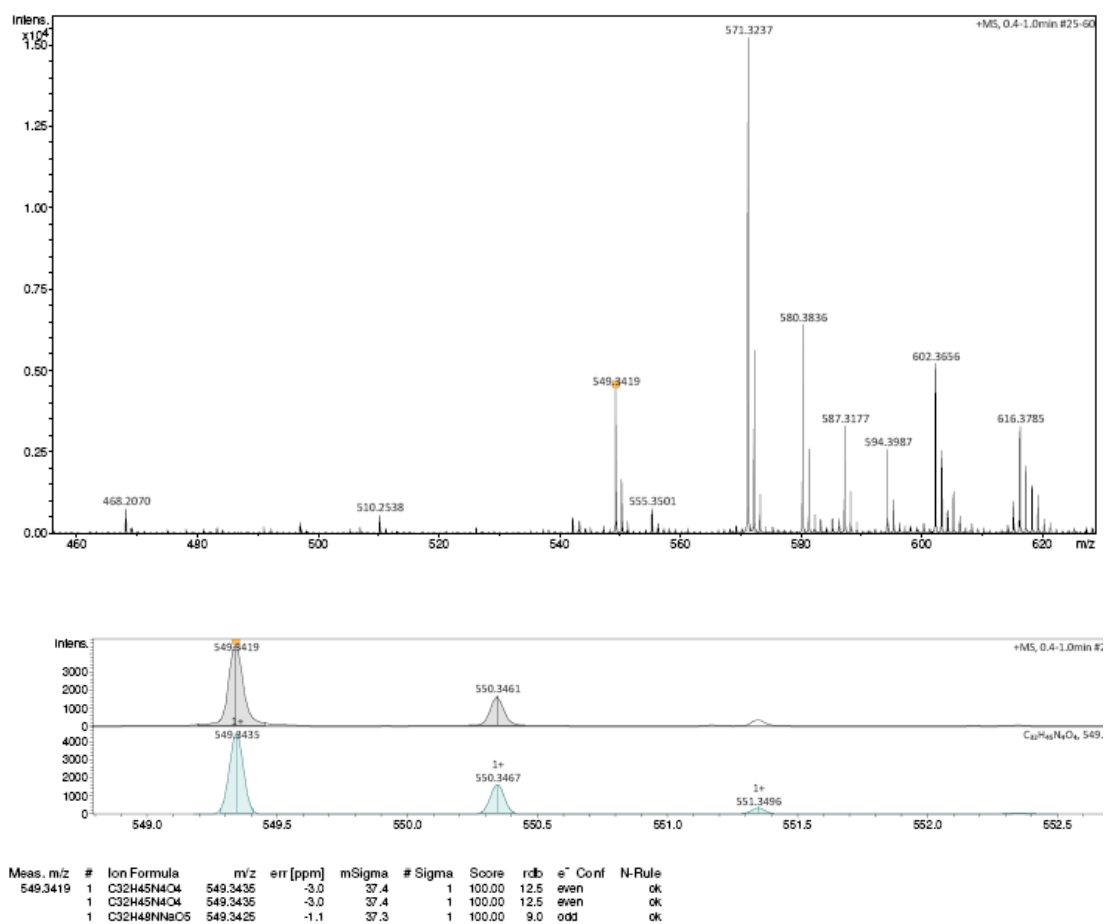


Figure S31. HRMS profile of cyclo[Leu-NMePhe-Leu-NMePhe] (**6a**, **6b**)

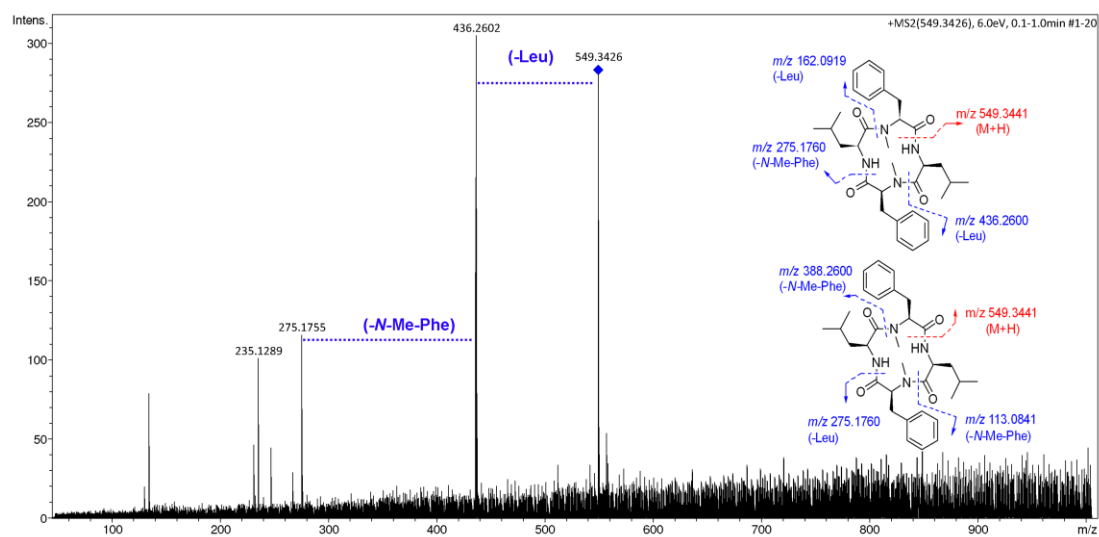


Figure S32. HRMS/MS profile of cyclo[Leu-NMePhe-Leu-NMePhe] (**6a**, **6b**)

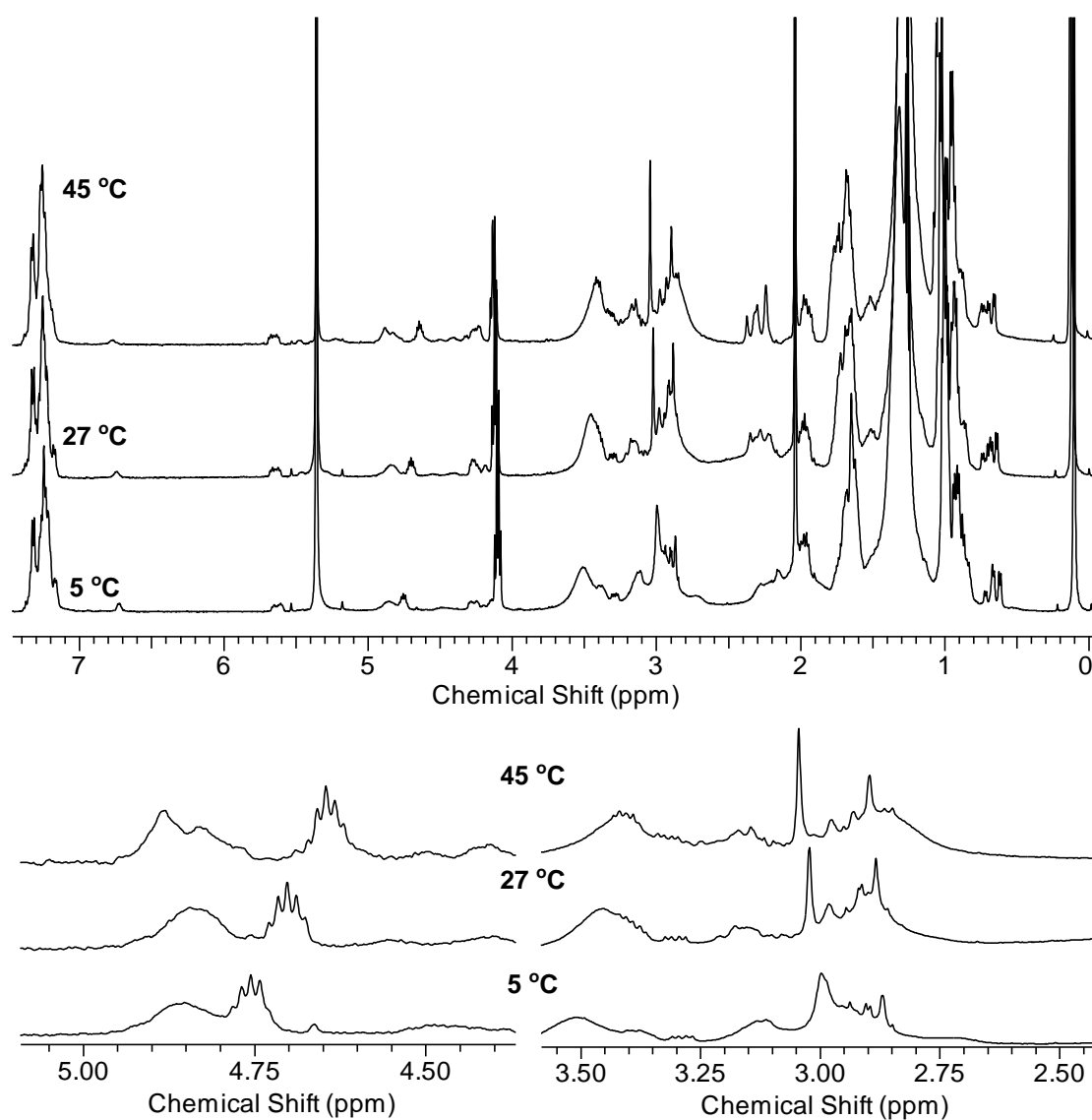


Figure S33. (Top) ¹H NMR spectra (500 MHz, CD₂Cl₂) of the cyclisation of **9** (2 mM) with T3P (1 equiv.) and DIPEA (3 equiv.) at 5, 27 and 45°C. (Bottom) Zoomed in of the above spectrum covering the C^αH and N-methyl proton regions from left to right.

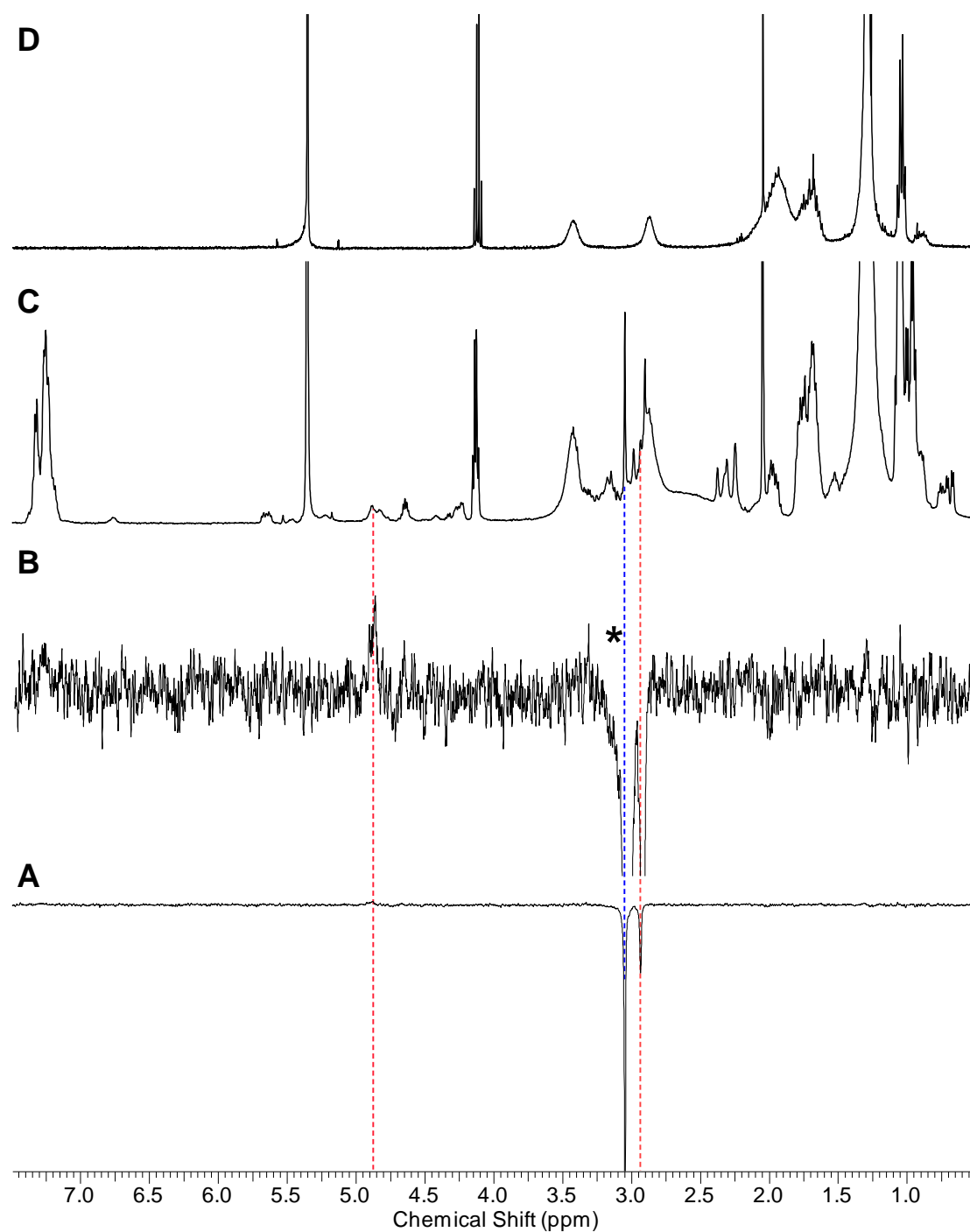


Figure S34. **A**) 1D NOE NMR spectra (500 MHz, CD_2Cl_2 , 27 °C) of the reaction mixture of **9** (2 mM), T3P (1 equiv.) and DIPEA (2 equiv.) in CD_2Cl_2 after 30 min at 5 °C. **B**) Magnified spectrum from **A**. * indicates the irradiating frequency. **C**) ^1H NMR spectra (500 MHz, CD_2Cl_2 , 27 °C) of the reaction mixture of **9** (2 mM), T3P (1 equiv.) and DIPEA (2 equiv.) in CD_2Cl_2 after 30 min. at 5 °C and **D**) of the mixture of T3P and DIPEA (1:2) in CD_2Cl_2 .

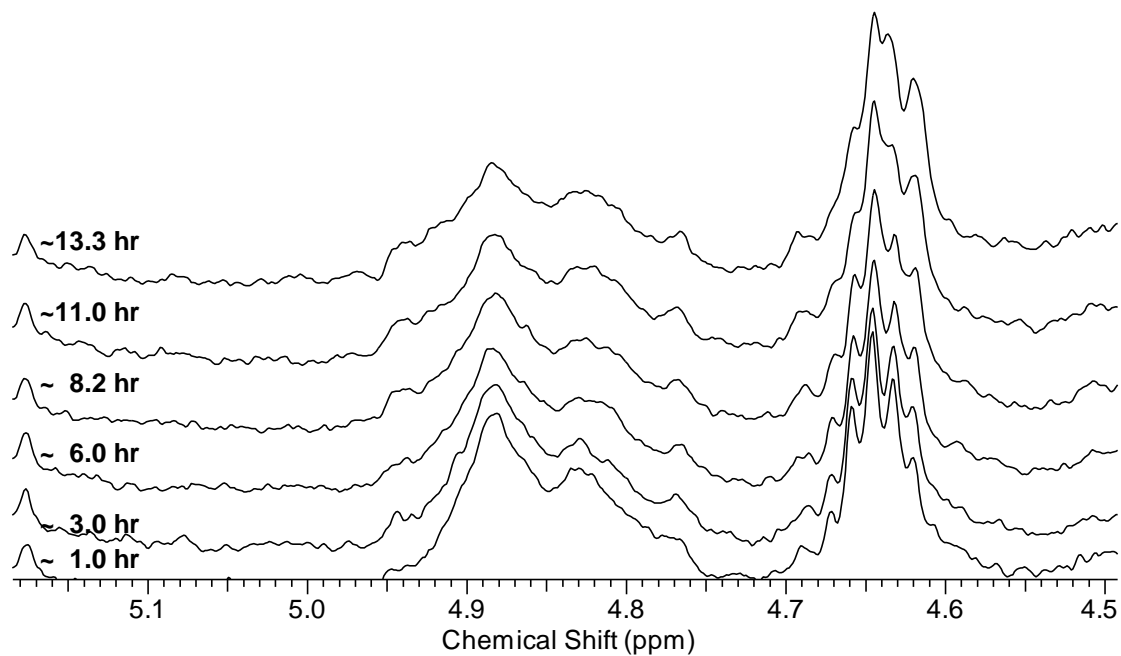


Figure S35. ¹H NMR spectra (500 MHz, CD₂Cl₂, 45 °C) of the reaction mixture of **9** (2 mM), T3P (1 equiv.) and DIPEA (2 equiv.) in CD₂Cl₂ at different time points. The spectrum shows the C^αH proton region.

Cyclo[Leu-NMePhe-Val-NMePhe] (7)

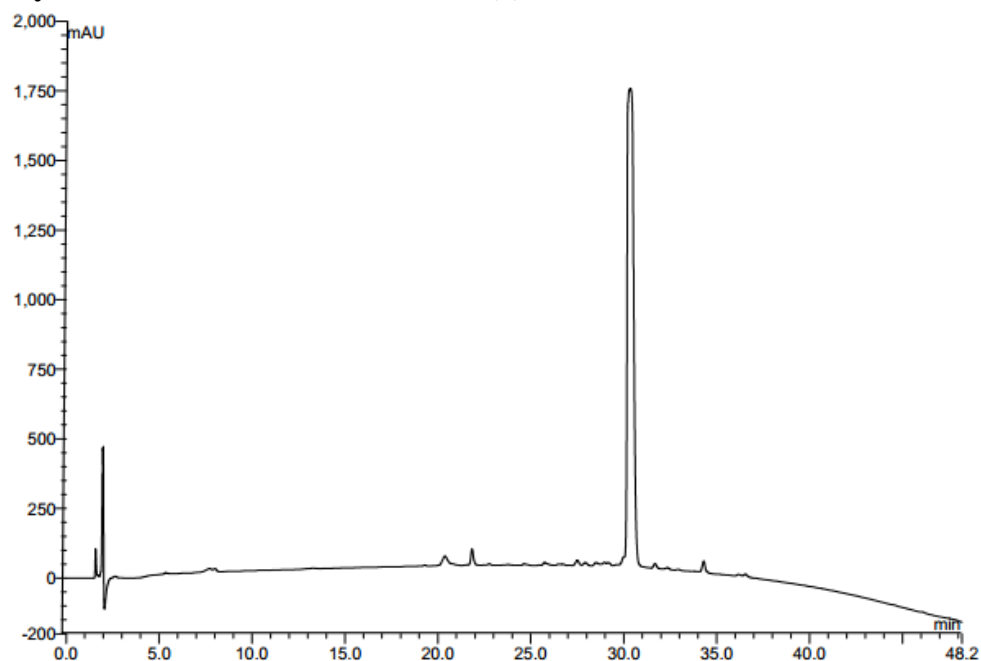


Figure S36. Analytical RP-HPLC profile of cyclo[Leu-NMePhe-Val-NMePhe] (7); linear gradient of 5%B-95%B over 45 min (*ca.* 2 %B \cdot min $^{-1}$), 1 mL \cdot min $^{-1}$, using XTerra MS C₁₈ column (4.6 mm \times 150 mm, 5 μ m).

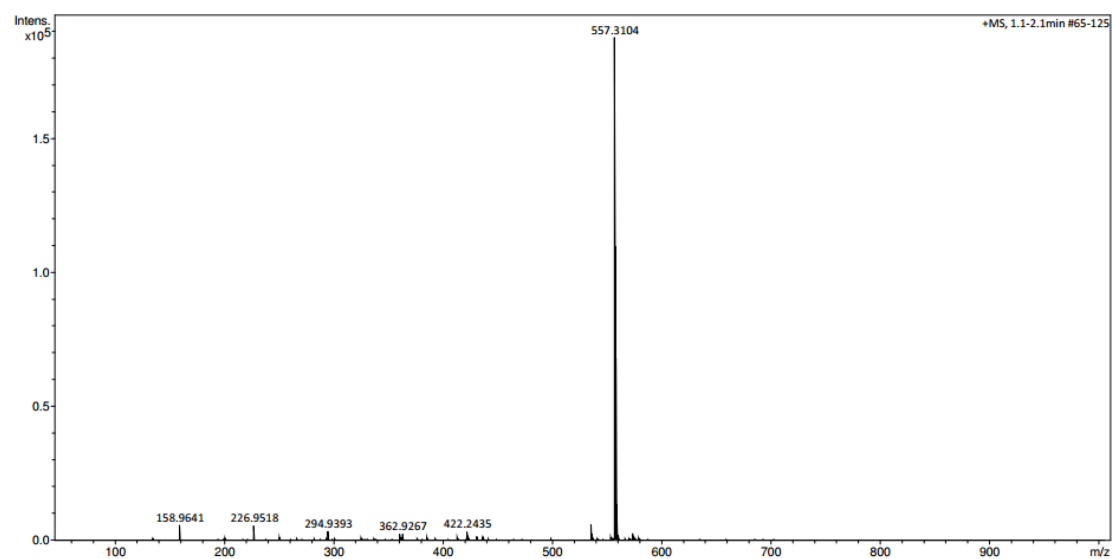


Figure.S37. HRMS profile of cyclo[Leu-NMePhe-Val-NMePhe] (7)

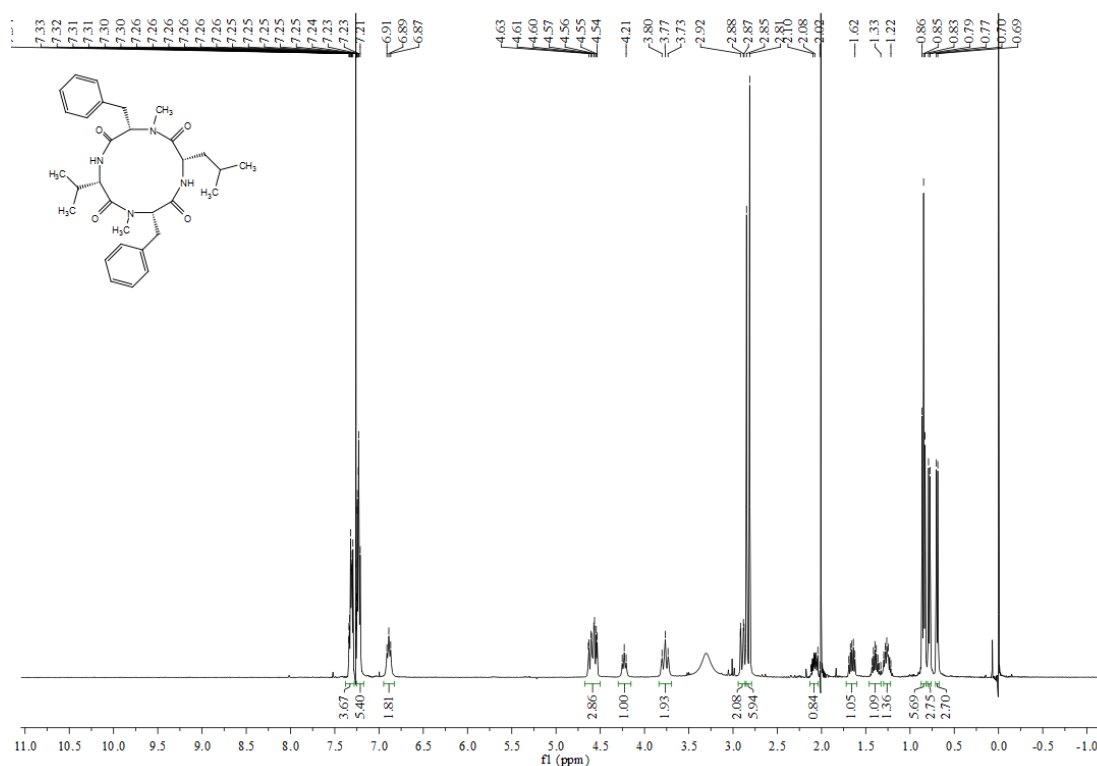


Figure.S38. ¹H NMR spectrum (400 MHz, CDCl₃) of cyclo[Leu-NMePhe-Val-NMePhe] (7)

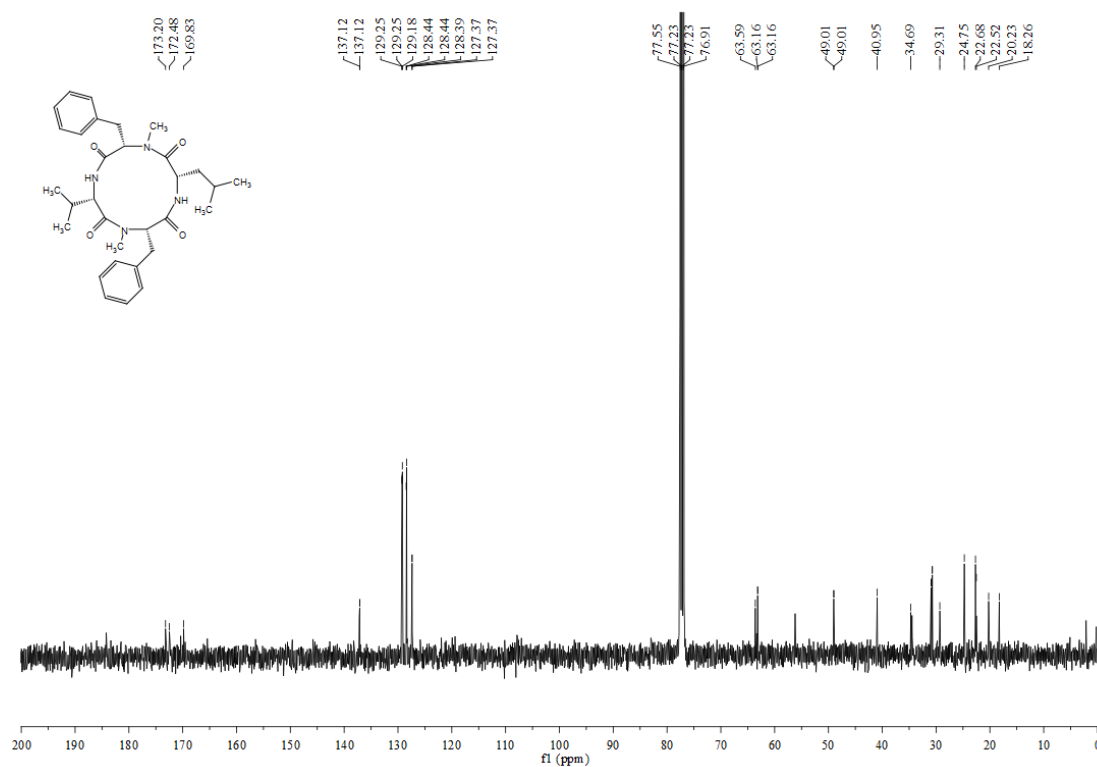


Figure.S39. ¹³C NMR spectrum (100 MHz, CDCl₃) of cyclo[Leu-NMePhe-Val-NMePhe] (7)

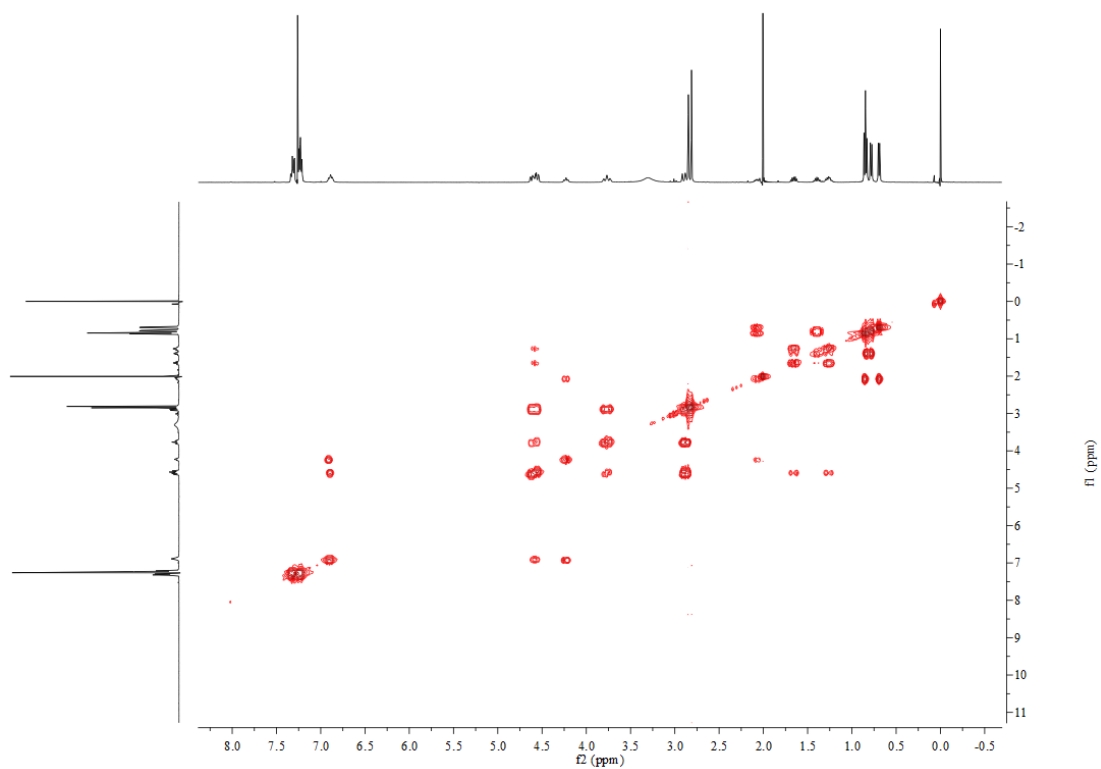


Figure S40. COSY spectrum (400 MHz, CDCl_3) of cyclo[Leu-*N*MePhe-Val-*N*MePhe] (7)

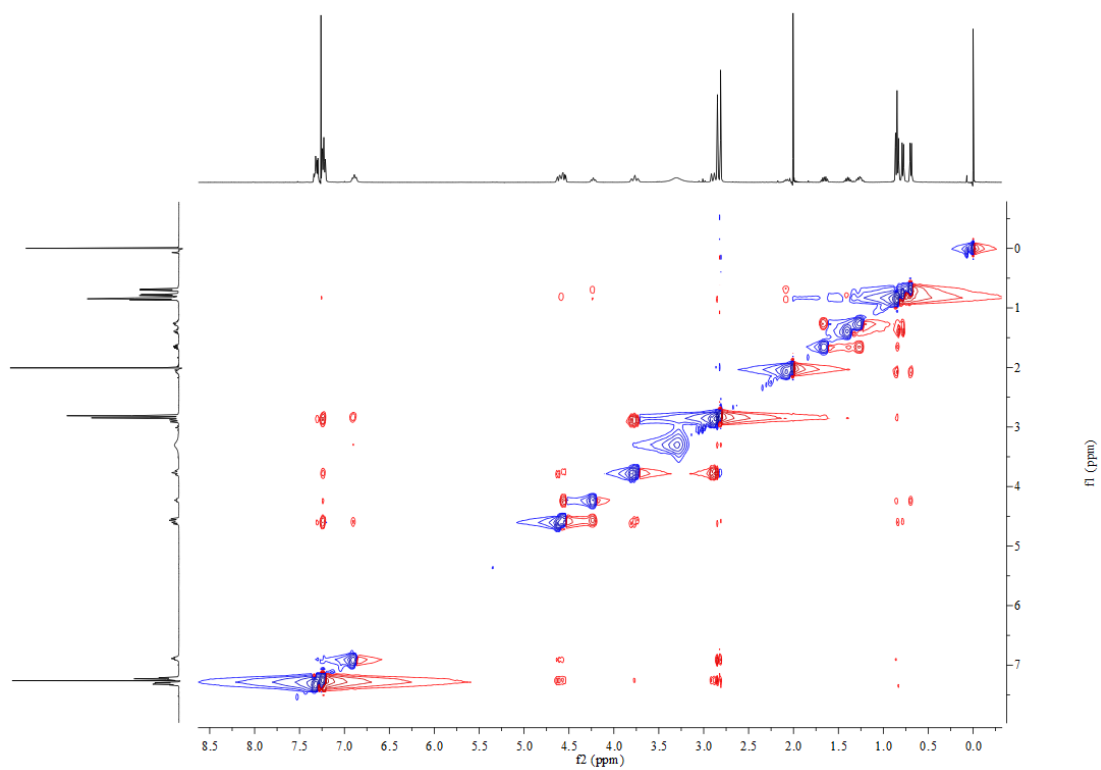
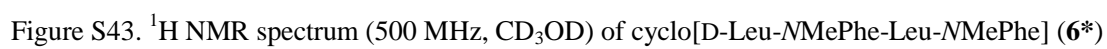
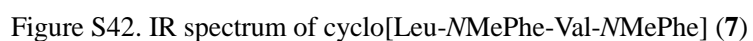


Figure S41. NOESY spectrum (400 MHz, CDCl_3) of cyclo[Leu-*N*MePhe-Val-*N*MePhe] (7)



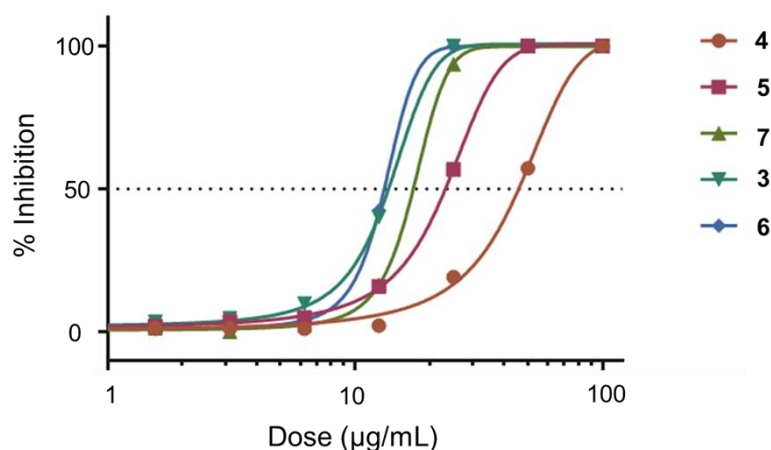


Figure S44. The dose-dependent inhibition of five cyclotetrapeptides against mouse myeloma cells.

Table S1. Optimized structures of the different conformers of **6*** in a tube representation (top). Potential energy differences relative to the *tctc* conformer (in kcal/mol) and dipole moments (given in parenthesis in Debye) of the three minimised conformers of **6** in *vacuum*, DMSO and CH₂Cl₂.

	<i>tctc</i>	<i>ttct-1</i>	<i>ttct-2</i>	<i>tttt</i>	
	<i>tctc</i> (ΔPE ^a /μ ^b)	<i>ttct-1</i> ^c (ΔPE/μ)	<i>ttct-2</i> ^d (ΔPE/μ)	<i>tttt</i> (ΔPE/μ)	6 (ΔPE/μ)
Vacuum	6.40/2.20	14.40/1.05	11.48/4.62	11.59/4.49	0 ^e /0.21
DMSO	4.37/4.55	13.65/1.65	10.90/7.94	12.98/7.46	0 ^e /1.33
CH ₂ Cl ₂	4.32/4.23	13.75/1.44	11.32/6.95	12.71/6.83	0 ^e /0.96

[a] ΔPE: Potential energy difference (kcal/mol). [b] μ: Dipole moment. [c] *ttct* conformer containing a *cis* amide bond between D-Leu and NMe-Phe. [d] *ttct* conformer containing a *cis* amide bond between Leu and NMe-Phe. [e] The absolute potential energy for **6** in *vacuum*, DMSO and CH₂Cl₂ is -1108149.20, -1108162.45 and -1108160.10 kcal/mol, respectively.

Table S2. Potential energy (in kcal/mol) and dipole moments (given in parenthesis in Debye) of the three minimised conformers of **6** in *vacuum*, DMF and CH₂Cl₂.

	<i>tttt</i> (PE ^a /μ ^b)	<i>tttc</i> (PE/μ)	<i>tctc</i> (PE/μ)
Vacuum	-56.376/0.80	-58.826/4.66	-65.479/0.34
DMSO	-69.742/0.75	-73.750/4.83	-85.383/0.39

CH₂Cl₂ -68.659/0.74 -79.234/4.37 -83.407/0.37

^aPE: Potential energy; ^bμ: Dipole moment.